Supercharged cellulases show superior thermal stability and enhanced activity towards pretreated biomass and cellulose

Bhargava Nemmaru^{a,#}, Jenna Douglass^{a,#}, John M Yarbrough^b, Antonio DeChellis^a, Srivatsan
 Shankar^a, Alina Thokkadam^a, Allan Wang^a, Shishir P. S. Chundawat^{a,*}

^a Department of Chemical & Biochemical Engineering, Rutgers The State University of New
 Jersey, Piscataway, New Jersey 08854, USA.

^b Biosciences Center, National Renewable Energy Lab, Golden, Colorado 80401, USA.

Corresponding Author Name: Shishir P. S. Chundawat* (ORCID: 0000-0003-3677-6735)

Corresponding Author Email: shishir.chundawat@rutgers.edu

111213

14

15

16 17

18 19

20

21

22 23

24

25

26 27

28

29

30 31

32

33

34 35

36

10

7

8 9

1

2

ABSTRACT: Non-productive binding of cellulolytic enzymes to various plant cell wall components, such as lignin and cellulose, necessitates high enzyme loadings to achieve efficient conversion of pretreated lignocellulosic biomass to fermentable sugars. Protein supercharging was previously employed as one of the strategies to reduce non-productive binding to biomass. However, various questions remain unanswered regarding the hydrolysis kinetics of supercharged enzymes towards pretreated biomass substrates and the role played by enzyme interactions with individual cell wall polymers such as cellulose and xylan. In this study, CBM2a (from *Thermobifida fusca*) fused with endocellulase Cel5A (from *Thermobifida* fusca) was used as the model wild-type enzyme and CBM2a was supercharged using Rosetta, to obtain 8 variants with net charges spanning -14 to +6. These enzymes were recombinantly expressed in E. coli, purified from cell lysates, and their hydrolytic activities were tested against pretreated biomass substrates (AFEX and EA treated corn stover). Although the wild-type enzyme showed greater activity compared to both negatively and positively supercharged enzymes towards pretreated biomass, thermal denaturation assays identified two negatively supercharged constructs that perform better than the wild-type enzyme (~3 to 4-fold difference in activity) upon thermal deactivation at higher temperatures. To better understand the causal factor of reduced supercharged enzyme activity towards AFEX corn stover, we performed hydrolysis assays on cellulose-I/xylan/pNPC, lignin inhibition assays, and thermal stability assays. Altogether, these assays showed that the negatively supercharged mutants were highly impacted by reduced activity towards xylan whereas the positively supercharged mutants showed dramatically reduced activity towards cellulose and xylan. It was identified that a combination of impaired cellulose binding and lower thermal stability was the cause of reduced hydrolytic activity of positively supercharged enzyme sub-group. Overall, this study demonstrated a systematic approach to investigate the behavior of supercharged enzymes and

[#] Equal contribution

^{*}Corresponding Author: Shishir P. S. Chundawat (<u>shishir.chundawat@rutgers.edu</u>, Tel: 848-445-3678)

- 1 identified supercharged enzyme constructs that show superior activity at elevated temperatures.
- 2 Future work will address the impact of parameters such as pH, salt concentration, and assay
- 3 temperature on the hydrolytic activity and thermal stability of supercharged enzymes.

KEYWORDS: Cellulase, Carbohydrate-binding module, Computational protein design, Thermal stability, Enzyme supercharging, Lignin inhibition, Non-productive binding, Cellulosic biomass hydrolysis

INTRODUCTION

The future circular economy is based on conversion of wastes from a variety of streams to useful products that are currently produced from fossil fuels^{1,2}. Bioethanol is one such product that can be produced from lignocellulosic biomass such as agricultural residues (e.g., corn stover, wheat/rice straws, sugarcane bagasse) and forest residues (e.g., wood chips)³. The versatility of available biomass sources and the variety of bioproducts that can be generated, lends itself to development of customized conversion strategies tailor-made for various feedstocks in an integrated biorefinery^{4,5}. One conversion strategy that has received significant attention is the enzymatic conversion of cellulose and hemicellulose to C6/C5 based mixed sugar streams³, while employing tailored valorization strategies for extracted lignin based on the pretreatment strategy^{6,7}. These sugars can be converted to a variety of platform chemicals such as ethanol, organic acids, or polymer-precursors in an integrated biorefinery⁸.

Various techno-economic analyses have been performed to assess the feasibility of producing bioethanol in a cost-effective and sustainable manner from biomass^{9,10}. These studies have highlighted the role of high enzyme costs prohibiting commercialization of biofuels¹¹. Hence, there is a need to develop enzyme engineering strategies to improve the overall conversion of lignocellulosic biomass to reducing sugars, while reducing biomass recalcitrance via thermochemical pretreatment^{12,13}. Non-productive binding of enzymes to lignin and cellulose along with limited enzyme accessibility to the substrate are considered the key factors that limit enzyme activity towards pretreated biomass substrates^{14–17}. As a result, pretreatment efforts have focused on extraction of lignin for valorization while also improving overall enzyme accessibility to the residual polysaccharides^{18,19}.

 However, most modes of pretreatment technologies (e.g., dilute acid, extractive ammonia, alkaline, deacetylation and mechanical refining or DMR) only extract lignin partially, leaving behind residual lignin that can still deactivate or inhibit enzymes^{20,21}. Lignin has been shown to deactivate cellulases through various mechanisms, the most significant of which involves protein conformational changes upon adsorption to lignin driven via hydrophobic interactions^{22–24}. Broadly speaking, the three strategies that have been employed to reduce cellulase non-productive binding to lignin include: (i) addition of sacrificial proteins such as BSA²⁵ or soy protein,²⁶ (ii) inclusion of negatively charged groups such as acetyl groups on the surface of enzymes via chemical conjugation,²⁷ and (iii) enzyme surface supercharging via computational re-design^{28,29}. Although the first two strategies have been shown to reduce lignin

inhibition, they require an additional reagent (BSA or soy protein) or treatment procedure (acetylation), which increases the operating or capital cost of the bioconversion process. On the other hand, enzyme supercharging is an inexpensive method of genetically engineering enzymes to alter their surface electrostatic properties^{30,31}.

 Protein supercharging has been used to accomplish a variety of useful applications including but not limited to macromolecule or drug delivery into mammalian cells³², DNA detection and methylation analysis³³, complex coacervation with polyelectrolytes³⁴, self-assembly into organized structures³⁵ such as protein nanocages³⁶ and Matryoshka-type structures³⁷ and encapsulation of cargo proteins into such higher-order structures³⁸. Previously, we have utilized a supercharging strategy based on Rosetta^{39,40} and FoldIt standalone interface⁴¹ for engineering green fluorescent protein (GFP)²⁸ and CelE (from Ruminiclostridium thermocellum)²⁹. We found that net negative charge was correlated weakly with reduced lignin binding capacity for GFP supercharged mutants, whereas the charge density was not found to have a clear impact on lignin binding capacity²⁸. In our follow-up study²⁹, a cellulase catalytic domain CelE was fused with CBM3a and both domains were individually negatively supercharged. Negatively supercharged CBM3a designs showed relatively improved hydrolysis yields on model amorphous cellulose in the presence of lignin, compared to the wild-type enzyme. However, all tested designs showed reduced absolute activity than wild-type controls on amorphous cellulose substrates (and with no data reported on pretreated lignocellulosic biomass) which was hypothesized to be due to reduced binding to cellulose induced by electrostatic repulsions.

Although these studies show proof-of-concept for the potential beneficial impact of cellulase negative supercharging on biomass hydrolysis, there remain multiple unanswered mechanistic questions to fully leverage the potential of enzyme supercharging for lignocellulosic biomass hydrolysis. Broadly speaking, there are three unanswered questions: (i) how does supercharging impact enzyme kinetics on pretreated biomass substrates? (ii) how can biomass hydrolysis performance of mutant enzymes be rationalized by understanding the activity and binding on individual polymers (cellulose, xylan, and lignin)? (iii) how does supercharging impact thermal stability and cellulase function at elevated temperatures? Here, we sought to address these questions in greater detail, using a model endocellulase enzyme Cel5A from *Thermobifida fusca (T. fusca)*, which has been well-characterized in our lab previously⁴². *T. fusca* is a thermophilic microbe that secretes cellulase enzymes belonging primarily to glycosyl hydrolase (GH) families 5, 6, 9, and 48, with most cellulase CDs tethered to a type-A CBM2a⁴³. Testing the protein supercharging strategy on a model Cel5A enzyme and its CBM2a from this cellulolytic enzyme system will also allow for extension of these design principles to other enzymes, potentially leading to a supercharged cellulase mixture with superior performance.

More specifically, we computationally designed a library of eight CBM2a designs spanning a net charge range of -14 to +6. These CBM2a designs were fused with the Cel5A catalytic domain and green fluorescent protein (GFP) separately, to study the hydrolysis activity and binding behavior of the constructs on a variety of substrates, respectively. Firstly, we

characterized the hydrolysis yields of CBM2a-Cel5A fusion constructs at various reaction times (2-24 hours) on ammonia fiber expansion (AFEX) and extractive ammonia (EA) pretreated corn stover substrates. To further rationalize the activity of supercharged enzymes towards pretreated biomass substrates, we assayed enzyme activity towards cellulosic substrates and xylan. Moreover, we performed binding assays to study the binding of GFP-CBM2a fusion constructs to cellulose using previously established QCM-D assay procedures^{17,28}. We followed it up with thermal shift assays to measure melting temperatures of supercharged enzymes and tested enzyme activity upon thermal deactivation at elevated temperatures. Overall, this study presents a rational approach to understand the mechanistic underpinnings of supercharged enzyme action on pretreated biomass substrates by deconvoluting the impact of cellulose and xylan hydrolysis and thermal stability.

EXPERIMENTAL SECTION

Reagents: AFEX and EA pretreated corn stover were prepared and provided in kind by Dr. Rebecca Ong's lab (Michigan Technological University, Houghton) and Bruce Dale's lab (Michigan State University, East Lansing), according to previously established protocols^{44–46}. Avicel (PH 101, Sigma-Aldrich, St Louis) was used to prepare cellulose-III allomorph with the following pretreatment conditions (90 °C, 6:1 anhydrous liquid ammonia to cellulose loading, and 30 minutes of total residence time) and phosphoric acid swollen cellulose (PASC) as described previously⁴⁷. Sarvada Chipkar from the Ong lab kindly prepared and provided cellulose-III used in this study. Lignin extracted from corn stover was prepared using the organosolv extraction process⁴⁸ and kindly provided by Stuart Black of the National Renewable Energy Laboratory (NREL). All other chemicals and analytical reagents were procured either from Fisher Scientific or Sigma Aldrich, or as noted in the relevant experimental section.

Mutant energy scoring using Rosetta: Creation of computational designs carrying a certain net charge necessitated computing the change in energy scores upon mutation of a native amino acid residue to either a positively charged (K, R) or a negatively charged residue (D, E). These mutations were scored using Rosetta. The wild-type protein PDB file is obtained either via homology modeling using Rosetta CM⁴⁹ or via the protein data bank⁵⁰. PyMOL (Schrodinger) was used to generate the desired mutation in amino acid sequence of a given protein and exported as a PDB file that represents the mutated protein. Customized scripts were developed in Rosetta to perform fast relax⁵¹ of any input PDB file. PDB files of both the wild-type and mutated proteins were relaxed separately using ten fast relax operations at a time. Each round of energy minimization enabled by ten fast relax operations was repeated until the Rosetta energy score of protein equilibrated and did not vary by more than 0.1 Rosetta Energy Units (REU) between one round of energy minimization (comprising of 10 fast relaxes) to another. The mutation energy score for a given mutation was calculated by measuring the difference between Rosetta energy scores of the wild-type protein and the mutant after energy minimization.

Plasmid generation, protein expression and purification: Thermobifida fusca native 1 Cel5A^{52,53} (UniprotKB - O01786) gene was cloned into pET28a(+) (Novagen) and was kindly 2 provided by Nathan Kruer-Zerhusen (from late Prof. David Wilson's lab at Cornell University). 3 An N-terminal 8X His tag was inserted and the native signal peptide removed from the original 4 gene construct. The gene was then cloned into our in-house expression vector pEC to optimize 5 protein expression yields as described previously^{54,55}. The plasmid maps for pEC-CBM2a-6 Cel5A and pEC-GFP-CBM2a are provided in SI Appendix Figures S1 and S2 respectively. 7 The full nucleotide sequences with color coding for each gene segment are reported in the 8 supplementary file titled SI Appendix Sequences.docx. CBM2a mutant designs were 9 ordered from Integrated DNA Technologies, Inc (IDT) as custom-synthesized gBlocks. These 10 CBM2a design gBlocks were then swapped with wild-type CBM2a to generate mutant 11 CBM2a-Cel5A fusion constructs using standard sequence and ligation independent cloning 12 (SLIC) protocols. A similar approach was used to insert CBM2a designs into previously 13 reported pEC-GFP-CBM vector⁵⁵. Molecular cloning for *Thermobifida fusca* β-glucosidase 14 (UniprotKB - Q9LAV5) gene These colonies were then inoculated in LB medium and grown 15 overnight to prepare 20% glycerol stocks for long-term storage at -80 °C. These glycerol stocks 16 were then used to inoculate 25 ml of LB media with 50 µg/ml kanamycin and incubated at 37 17 18 ^oC, 200 rpm for 16 hours. These overnight cultures were then transferred to 500 ml autoinduction medium (TB+G)56 and incubated at 37 °C, 200 rpm for 6 hours to allow optical 19 density to reach the exponential regime. Protein expression was then induced by reducing the 20 temperature to 25 °C for 24 hours at 200 rpm. Cell pellets were then harvested using Beckman 21 22 Coulter centrifuge and JA-14 rotor by spinning the liquid cultures in 250 ml plastic bottles at 30,100 g for 10 minutes at 4 °C. All the cell culturing experiments were performed using an 23 Eppendorf InnovaTM incubator shaker. Cell pellets were lysed using 15 ml cell lysis buffer (20 24 mM phosphate buffer, 500 mM NaCl, 20% (v/v) glycerol, pH 7.4), 0.5 mM Benzamidine 25 (Calbiochem 199001), 200 ul protease inhibitor cocktail (1 uM E-64 (Sigma Aldrich E3132), 26 15 µl lysozyme (Sigma Aldrich, USA) and 1 mM EDTA (Fisher Scientific BP1201)) for every 27 3 g wet cell pellet. The cell lysis mixture was sonicated using MisonixTM sonicator 3000 for 5 28 29 minutes of total process time at 4.5 output level and specified pulse settings to avoid sample overheating (pulse-on time: 10 seconds and pulse-off time: 30 seconds). An Eppendorf 30 centrifuge (5810R) with F-34-6-28 rotor was then used to separate the cell lysis extract from 31 32 insoluble cellular debris at 15,500 g, 4 °C for 45 minutes. Immobilized metal affinity chromatography (IMAC) using His-Trap FF Ni⁺²-NTA column (GE Healthcare) attached to 33 BioRadTM NGC system, was then performed to purify the his-tagged proteins of interest from 34 35 the background of cell lysate proteins. Briefly, there were three steps involved during IMAC purification: 1. equilibration of column in buffer A (100 mM MOPS, 500 mM NaCl, 10 mM 36 Imidazole, pH 7.4) at 5 ml/min for 5 column volumes, 2. soluble cell lysate loading at 2 ml/min, 37 38 and 3. His-tagged protein elution using buffer B (100 mM MOPS, 500 mM NaCl, 500 mM Imidazole, pH 7.4). The purity of eluted proteins was validated using SDS-PAGE before buffer 39 exchange into 10 mM sodium acetate (pH 5.5) buffer for long-term storage after flash freezing 40 at -80 °C and/or follow-on activity characterization. 41 42

3

4

5 6

7

8

9

10

11

12 13

14

15

16 17

18

19

20

2122

23

24

25 26

27

28

29

30

31 32

33

34 35

36

37 38

39

40

41 42 Pretreated lignocellulosic biomass hydrolysis assays: AFEX and EA corn stover (milled to 0.5 mm) were suspended in deionized water to obtain slurries of 25 g/l total solids concentration. All biomass hydrolysis assays were performed in 0.2-ml round-bottomed microplates (PlateOneTM), with at least 4 replicates for each reaction condition. Reactions quenched at different time points (2, 6 and 24 hours) were performed in different microplates. Each reaction was composed of 80 µl biomass slurry (25 g/l), 20 µl sodium acetate buffer (0.5 M), 50 μl cellulase enzyme (at appropriate concentration), 25 μl β-glucosidase (at appropriate concentration), and 25 µl of deionized water to make up the total reaction volume to 200 µl. For reaction blanks, the enzyme solutions were replaced with deionized water while biomass slurry and buffer volumes remained the same. The cellulase enzyme loading was maintained at 120 nmol per gram biomass substrate and the β-glucosidase enzyme loading was maintained at 12 nmol per gram biomass substrate (leading to 10% of cellulase enzyme concentration). Since supercharged constructs have varying molecular weights, a molar basis was used for all hydrolysis assays to keep concentrations between enzymes normalized. A conversion of enzyme loading for each concentration to a mass basis can be viewed in the supplementary appendix. Upon addition of all the requisite reaction components, the microplates were covered with a plate mat, sealed with packaging tape, and incubated at 60 °C for the specified time duration (2, 6 or 24 hours) with end-over-end mixing at 5 rpm in a VWR hybridization oven. Upon reaction completion, the microplates were centrifuged at 3900 rpm for 10 minutes at 4 °C to separate the soluble supernatant (comprised of soluble reducing sugars) from insoluble biomass substrate. The supernatants were then recovered and dinitrosalicylic acid (DNS) assays were performed as previously described to estimate total soluble reducing sugars⁴². This data was fitted to a two-parameter kinetic model that was previously deployed to study reaction kinetics of *T. fusca* cellulases on biomass substrates⁵⁷. Origin software was used to perform the curve fitting analysis and obtain the pseudo-kinetic time-dependent parameters 'A' and 'b' which represent the net activity of bound enzyme and the time-dependent ability of enzyme to overcome recalcitrance, respectively. An increase in b might indicate the ability of enzyme to sample new substrate sites as reaction progresses, thereby reducing substrate recalcitrance.

Cellulose hydrolysis assays and lignin inhibition assays: The cellulose hydrolysis assays were performed in a similar manner as biomass hydrolysis assays, except for the reaction composition. Avicel PH101 derived cellulose-I and cellulose-III were suspended in deionized water to form slurries of 100 g/l total solids concentration. A 0.2-ml round-bottomed microplate (PlateOneTM) was used for each discrete reaction timepoint (2, 6 and 24 hours) and each reaction was performed with at least 4 replicates. Each reaction was composed of 40 μ l cellulose slurry (100 g/l), 20 μ l sodium acetate buffer (0.5 M, pH 5.5), 50 μ l cellulase enzyme (at appropriate concentration), 25 μ l β -glucosidase (at appropriate concentration) and 65 μ l of deionized water to make up the total reaction volume to 200 μ l. The cellulase enzyme loading was maintained at 120 nmol per gram biomass substrate and the β -glucosidase enzyme loading was maintained at 12 nmol per gram biomass substrate (leading to 10% of cellulase enzyme concentration). Upon reaction completion, supernatants were removed, and DNS assays were performed as described in the previous section on biomass hydrolysis assays. The reaction

mixture for lignin inhibition assays was composed of 20 μ l cellulose slurry (100 g/l), 40 μ l lignin slurry (20 g/l), 20 μ l sodium acetate buffer (0.5 M, pH 5.5), 50 μ l cellulase enzyme (at appropriate concentration), 25 μ l β -glucosidase (at appropriate concentration) and 65 μ l of deionized water to make up the total reaction volume to 200 μ l. The enzyme loadings and all the follow-on steps were conducted in a similar manner to cellulose hydrolysis assays. 24 hours was used as the preferred reaction time for lignin inhibition assays, owing to the prevalence of lignin and cellulose non-productive binding at longer reaction times.

Xylan hydrolysis assays: The xylan hydrolysis assays were performed in a similar manner as biomass hydrolysis assays, with a slight change to the reaction composition. Beechwood xylan suspended in deionized water to form slurries of 100 g/l total solids concentration. Equipment, procedures and reaction timepoint remained the same. Each reaction was composed of 20 μl xylan slurry (100 g/l), 20 μl sodium acetate buffer (0.5 M, pH 5.5), 50 μl cellulase enzyme (at appropriate concentration), 25 μl β-glucosidase (at appropriate concentration) and 85 μl of deionized water to make up the total reaction volume to 200 μl. The cellulase enzyme loading was maintained at 120 nmol per gram xylan substrate and the β-glucosidase enzyme loading was maintained at 12 nmol per gram biomass substrate (leading to 10% of cellulase enzyme concentration). All the follow-on steps were conducted in a similar manner to biomass hydrolysis assays.

pNPC kinetic hydrolysis assays: The pNPC hydrolysis assays were adapted from previously established protocols laid out in Whitehead et al. (2017). The assay was conducted in a 0.2-ml flat-bottomed clear microplate (PlateOneTM) and the enzyme activity was tested at pH 5.5 and pH 7.5. Each reaction was composed of 100 μ l pNPC slurry (2 mM), 7.5 μ l 1 M sodium acetate buffer pH 5.5 or 7.5 μ l 1 M MOPS (pH 7.5), 42.5 μ l cellulase enzyme (at an appropriate concentration to constitute 5 ug of enzyme per g pNPC). The reaction was performed for a duration of up to 700 minutes and the progress of hydrolysis reaction was tracked via pNP absorbance through a UV-vis spectrophotometer.

 Quartz crystal microbalance with dissipation (QCM-D) based binding assays: Preparation of cellulose and lignin films for characterization of GFP-CBM binding, was performed as described elsewhere 17,58 . Quartz sensors functionalized with nanocrystalline cellulose or lignin were mounted on the sensor holder of QSense E4 instrument and equilibrated with buffer (50 mM sodium acetate, pH 5.5 with 100 mM NaCl) for 10 minutes at a flow rate of 100 μ l/min using a peristaltic pump. The films were left to swell in buffer overnight and the films were considered stable if the third harmonic reached a stable baseline after overnight incubation. GFP-CBM2a protein stocks were then diluted to a concentration of 2.5 μ M using 50 mM sodium acetate (pH 5.5) and flown over the sensors at a flow rate of 100 μ l/min for 10 – 15 minutes until the system reached saturation, as observed by the third harmonic. The system was then allowed to equilibrate for at least 30 minutes and protein unbinding was then tracked by flowing buffer (50 mM sodium acetate, pH 5.5 with 100 mM NaCl) over the sensors at a flow rate of 100 μ l/min for at least 30 minutes. Data analysis for QCM-D traces was performed

as described previously¹⁷. However, for lignin, binding was observed to be mostly irreversible⁵⁹ and hence, only the maximum number of binding sites and percent irreversible protein bound, calculated based on the maximum number of binding sites and the amount of protein bound towards the end of unbinding regime.

Pretreated biomass/cellulose hydrolysis assays with thermally treated enzymes: This assay was performed in a similar way to the pretreated lignocellulosic biomass hydrolysis assays and the cellulose hydrolysis assays described above. However, the enzyme dilution used in those assay procedures was exposed to 70 °C in an Eppendorf thermocycler for 30 minutes followed by 10 °C for 10 minutes directly before being added into the microplate for reaction. The reaction was incubated for 60 °C for 24 hours only. The initial assay used all the enzyme designs with a denaturation temperature of 70 °C. From this the thermally stable enzyme designs, D1, D2 and the WT were exposed to temperatures of 73 °C, 76 °C, and 79 °C for 30 minutes prior to incubation at 60 °C for 24 hours.

Cellulase thermal shift assay: The protocol for thermal shift assays was similar to that reported previously²⁹. Briefly, 5 μl 200X SYPRO reagent, 5 μl 0.5 M sodium acetate buffer (pH 5.5), enzyme dilution to make up an effective concentration of 5 μM and deionized water to make up the total volume to 50 μl were added to MicroAmpTM EnduraPlateTM 96-well clear microplate (Applied BiosystemsTM). QuantStudio3 (Applied BiosystemsTM) was then used to measure the fluorescence using the channel allocated to FAM dye (excitation: 470 nm, emission: 520 nm) under a temperature ramp from 25 °C to 99 °C at a rate of 0.04 °C per second. The melting curves obtained were then analyzed using an open-source tool called SimpleDSFViewer⁶⁰.

RESULTS AND DISCUSSION

 Selection of a wild-type construct from CBM family 2 for supercharging: CBM family 2 comprises a large collection of mostly bacterial CBMs, with ~ 11,000 entries and 10 solved structures. *T. fusca*, an industrially relevant cellulolytic microbe, secretes multi-modular cellulase enzymes comprised of CBMs from family 2. Cel5A (endocellulase from GH5) was chosen as the model cellulase and tested for expression and activity, both with its native CBM2a and CBM2a from exocellulase Cel6B. The objective was to fuse each CBM to the Cel5A catalytic domain and identify the fusion enzyme that shows greater thermal stability as a target for supercharging. These two fusion cellulases are labeled as CBM2a (native) Cel5A and CBM2a (Cel6B) Cel5A from hereon. SI Appendix Figure S3 shows the hydrolytic activity of both enzyme constructs towards AFEX corn stover and cellulose-I. Surprisingly, CBM2a (Cel6B) Cel5A showed 1.8 to 2.5-fold improvement in activity towards both substrates compared to CBM2a (native) Cel5A, across all timepoints considered. This experiment was followed up with a measurement of enzyme activity upon thermal treatment at 70 °C, as reported in SI Appendix Figure S4. CBM2a (Cel6B) Cel5A loses ~ 60% of activity towards both substrates (AFEX corn stover and cellulose-I) whereas CBM2a (native) Cel5A loses up

to \sim 90% activity. The fusion of the cellulose binding module from CBM2a from Cel6B with the catalytic domain from Cel5A showed the greatest hydrolytic activity and thermal resistance. As a result, we chose CBM2a (Cel6B) Cel5A as the wild-type construct to be engineered in this study. CBM2a (Cel6B) Cel5A will be referred to as wild-type CBM2a Cel5A or WT for the remainder of this paper.

 Design of supercharged CBM2a library: A homology model was constructed for the target CBM2a (Cel6B) wild-type protein using Rosetta CM tool⁴⁹ based on templates from CBM family 2a with at least 50% sequence identity. Surface residues were then identified using an appropriate residue selector in Rosetta. Previous studies have shown that 10% of the total amino acid sequence length of globular proteins can be mutated using the supercharging strategy, while still allowing the proteins to fold properly³¹. Given that CBM2a is 100 amino acids long and has a net charge of -4, we sought to generate designs that spanned a net charge range of -14 to +6 using 10 mutations of polar uncharged amino acid residues. Overall, 31 polar uncharged amino acid residues were identified on the protein surface and these residues were scored individually for mutations to lysine (K), arginine (R), aspartic acid (D) and glutamic acid (E).

The mutation energy scores were then averaged for any given position and surface polar uncharged residues were sorted based on these average mutation energy scores. From the original pool of 31 polar uncharged residues, three categories of residues were considered immutable due to their potential implications for protein folding or interaction with cellulose as follows: 1. residues within 10 Å distance from evolutionarily conserved planar aromatic residues⁶¹ essential for CBM function, 2. residues on the CBM binding face⁶², and 3. residues with a positive average mutation energy score (predicting structural instability upon mutation). Upon exclusion of these three categories of residues, 11 mutable polar uncharged residues were identified and sorted into two spatially distinct clusters and sorted based on their mutation energy scores from highest to lowest. The individual and average mutation energy scores of mutable residues are reported in SI Appendix Table T1. Eight designs were then generated to have net charges of -14 (D1), -12 (D2), -10 (D3), -8 (D4), -6 (D5), -2 (D6), +2 (D7) and +6 (D8) as shown in Figure 1. Negatively supercharged space was sampled more granularly because negative supercharging has been shown to reduce lignin inhibition in our previous work²⁹. The mutations used to generate each design, are reported in SI Appendix Table T2 whereas the full amino acid sequence for wild-type CBM2a with these mutable residues highlighted in red font, are reported in a separate file titled 'SI Appendix Sequences.docx'.

Hydrolytic activities of supercharged CBM2a-Cel5A constructs towards pretreated biomass: All CBM2a-Cel5a designs were cloned, expressed, and purified as described in the experimental procedures section. The hydrolytic activity of the supercharged and wild type cellulases were tested against pretreated biomass, namely AFEX corn stover. The hydrolysis yields are reported in the form of glucose equivalent reducing sugars released at 3 time points (2 hours, 6 hours and 24 hours) resulting in reaction progress curves shown in **Figure 2.** Based

on the raw hydrolysis data reported in **Figure 2A**, the negatively supercharged and positively supercharged mutants were separated into two groups and their average hydrolysis yields were reported in **Figure 2B**.

> From Figure 2A, it is evident that the wild-type enzyme (WT) has the highest activity compared to any supercharged mutant. The wild-type showed ~ 1.2 to 1.8-fold greater activity compared to negatively supercharged mutants and ~ 1.5 to 24.1-fold greater activity compared to positively charged mutants. D6 was an outlier amongst the positively supercharged group, showing higher activity compared to D7 and D8 across all timepoints considered. Similar trends were observed with EA corn stover, another model pretreated biomass substrate, for which the hydrolysis yields are reported in a similar format in SI Appendix Figure S5. To further compare the hydrolysis yields of mutants on AFEX and EA corn stover, T-tests were performed between each mutant pair within the negatively supercharged (D1-D5) and positively supercharged (D6-D8) groups, as reported in SI Appendix Table T3. On AFEX corn stover, mutants within D1 – D5 group were found to not show statistically significant differences at 2 hours although certain mutant pairs showed p < 0.05 at 6 hours and 24 hours. Within D6 - D8, D6 showed statistically significant differences from D7 and D8 at most timepoints. To understand the behavior of each group compared to the wild-type, the activities of negatively supercharged mutants (D1 - D5) and positively supercharged mutants (D6 - D8)were averaged separately and reported in Figure 2B. Positively supercharged mutants ranked the least as a group, at every time point considered, followed by negatively supercharged mutants with the wild type consistently ranking higher than both.

The reaction kinetic data on AFEX and EA corn stover for each individual mutant was then fit to a two-parameter model as described previously (shown in SI Appendix Table T4). Parameter 'A' represents the net activity of the bound enzyme whereas parameter 'b' represents the enzyme's ability to reduce biomass recalcitrance over time. On AFEX corn stover, the wild-type showed ~ 0.8 to 1.5-fold improvement in parameter 'A' over the negatively supercharged enzymes and ~ 2 to 6-fold improvement over positively supercharged enzymes. D1 was the only mutant to show an improvement in 'A' over wild-type indicating that the net activity of bound enzyme for this mutant may have been greater than the wild-type but the mutant perhaps lacks the ability to access new binding sites that can reduce recalcitrance of the enzyme. Similar trends were observed for EA corn stover, with D1 being the only mutant to show improvement in A.

Since electrostatic interactions between supercharged mutants and biomass may be influenced by the presence of salt, a hydrolysis assay was run at the 2-hour timepoint in the presence of 100mM NaCl (see **SI Appendix Figure S6**). The presence of salt showed little to no impact for most mutants, except in the case of D7 on AFEX corn stover for which the presence of salt improved activity by more than 2-folds.

1 Overall, the wild type showed improved activity compared to all the supercharged mutants.

The trends observed for the different cellulases towards pretreated biomass could arise from a

combination of various factors: (i) cellulolytic activity, (ii) xylanolytic activity, (iii) lignin

4 interactions, or (iv) thermal stability. We designed specific assays to understand each of these

5 contributions to pretreated biomass hydrolysis as discussed below.

2

3

6 7

8

9

10

11

12

13

14

15

16 17

18

19 20

21

2223

24

25

26

27

28 29

30

31 32

33

34 35

36

37 38

40 41

42

Hydrolytic activities of supercharged CBM2a-Cel5A constructs towards cellulosic **substrates:** Hydrolysis yields for cellulose-I were measured in terms of reducing sugar release at three time points (2 hours, 6 hours and 24 hours) using 120 nmol enzyme per gram substrate loading, resulting in reaction progress curves shown in Figure 3A for Avicel Cellulose-I and SI Appendix Figure S7A for Avicel Cellulose-III. Cellulose-I and Cellulose-III were chosen as the target substrates because these are the predominant cellulose allomorphs that comprise AFEX corn stover and EA corn stover respectively. The wild-type showed activity that was ~ 0.8 to 1.2-folds compared to negatively supercharged mutants (D1 – D5) and \sim 0.9 to 4.5-folds that of positively supercharged mutants (D6 – D8). Unlike the trends observed towards pretreated biomass in the previous section, negatively supercharged mutants (D1 – D5) show either increased or comparable activities to the wild type. On cellulose-III, most negatively supercharged mutants performed better than the wildtype, as observed in SI Appendix Figure S7A. T-tests revealed that there were no statistically significant differences between each mutant pair in the negatively supercharged group (D1 - D5) or within the negatively supercharged group (D6 – D8), with a few exceptions (see SI Appendix Table T5). To understand the behavior of each group compared to the wild-type, the activities of negatively supercharged mutants (D1 – D5) and positively supercharged mutants (D6 – D8) were averaged separately and reported in Figure 3B and SI Appendix Figure S7B for Cellulose-I and Cellulose-III respectively. The two-parameter kinetic model fits, achieved as described for biomass, are reported for cellulose-I and cellulose-III in SI Appendix Table T6.

negatively supercharged mutants (D1 - D5) across both substrates. On the other hand, negatively supercharged mutants showed comparable performance to wild type in the case of cellulose-I and outperformed the wild type in the case of Cellulose-III. Combining these results along with trends observed towards pretreated biomass substrates in the previous section, it is evident that the reduced activity of negatively supercharged mutants towards AFEX and EA corn stover may be resulting from one of the other factors such as xylanolytic activity, interactions with lignin or thermal stability. Similar results were obtained in previous works

where a decrease in hydrolytic activity towards PASC was observed for negatively

Overall, positively supercharged mutants (D6 – D8) consistently ranked below wild type and

supercharged mutants.²⁹ However, the lower activity of positively supercharged mutants

towards cellulose may be one of the causal factors behind their overall lowered activity towards

39 pretreated biomass.

Hydrolytic activities of supercharged CBM2a-Cel5A constructs towards xylan and pNPC: Certain cellulases like Cel5A are multifunctional and exhibit activity on xylan, thus the

2

4

5 6

7

8

9

10

11

12

13

14

15

16 17

18 19 20

21

2223

24

25

26

27

28 29

30

31

32 33

34 35

36 37

38

39 40

41 42 mutants were screened for their activity towards beechwood xylan and the raw data is reported in Figure 4A These results show that the negatively supercharged mutants show reduced activity compared to the wild-type, with the difference becoming more prominent at longer hydrolysis durations such as 24 hours. Upon averaging the activities of all supercharged mutants of the same type (negative (D1 - D5) vs positive (D6 - D8)) as shown in **Figure 4B**, it is evident that the negatively supercharged mutants collectively show greater than 1.5-fold reduction in activity. The positively supercharged mutants also show a reduction in activity compared to the wild-type but their activity is very similar to that of negatively supercharged mutants. This is unlike the case of insoluble substrates such as AFEX corn stover or cellulose-I where the positively supercharged mutants showed demonstrably reduced activity compared to the wildtype and negatively charged subgroup. Surprisingly, the mutant D8 showed improved activity compared to the wild-type, despite showing drastically activity amongst the cohort, towards AFEX corn stover and cellulose-I. This trend could likely be due to the reduced significance of CBM function for soluble substrates such as Xvlan. Summarizing the results of activity towards biomass, cellulose and xylan, it can be inferred that the reduced activity of negatively supercharged mutants (D1 - D5) towards biomass arises predominantly from reduced activity towards Xylan. Positively supercharged mutants D7 and D8 show consistently reduced activity towards all substrates tested although they show activity similar to that of the

To validate these trends towards another model soluble substrate, we tested hydrolytic activity towards pNPC (see SI Appendix Figure S8). This assay was originally designed to test activity at pH 7.5 (as reported by Whitehead et al. (2017)); however, we adapted the assay to pH 5.5 to keep the pH consistent across all substrates tested in this study. The raw data reported in SI **Appendix Figure S8A, S8C** was analyzed further to obtain averages for each individual group (D1 – D5 and D6 – D8), which is reported in SI Appendix Figure S8B, S8D. At pH 5.5, all mutants show a negligible reduction in activity towards pNPC (SI Appendix Figure S8B) whereas at pH 7.5, negatively supercharged mutants on average showed improved activity compared to the wild-type (SI Appendix Figure S8D). Mutant D8 was amongst the top performers in the pNPC assay at pH 7.5, performing distinctly better than the other positively supercharged enzymes. Overall, the activity towards pNPC shows that in the case of positively supercharged mutants (D7 and D8 specifically), the structural integrity of cellulase enzyme may not have been affected in an adverse manner and that the reduced activities observed towards pretreated corn stover or cellulosic substrates may be a result of reduced binding interactions of CBMs to cellulose/lignin or an impact to thermal stability caused due to supercharging.

Binding of mutants to cellulose and lignin: To fully understand the role of CBM binding interactions on the activities of supercharged mutants towards cellulose and thereby pretreated biomass, we performed QCM-D assays (see **SI Appendix Figure S9** for raw data in the form of sensorgrams) which capture the total number of binding sites and the desorption rate constant (k_{off}) . As reported in **Table 1**, all mutants except for D5 and D6 showed comparable or a reduced number of binding sites (up to 1.5-fold as observed for D1) with respect to the

wild-type. D6 shows the highest binding of all mutants, showing up to 1.5-fold improvement, which could partially explain the higher activity seen for this mutant towards cellulose-I (see **Figure 3**) compared to other positively supercharged mutants D7 and D8. On the other hand, all mutants except for D5 and D8 show an improvement in (k_{off}) , with D2 showing the most improvement (~ 1.3 -fold). The most dramatic reduction was observed for D8, which has ~ 9 -fold reduction in k_{off} . These results could explain the large decrease in activity observed for D8 CBM2a-Cel5A toward cellulose-I and thereby AFEX corn stover.

> Lignin is a key polymer in pretreated biomass, which has the potential to restrict access to cellulose binding sites and thereby reduce overall biomass hydrolysis yields. QCM-D assays were performed to understand the binding of supercharged CBM2a mutants to lignin (see SI Appendix Figure S10 for raw data). As reported in SI Appendix Table T7, all mutants show an improvement in the percentage of protein recovered, indicating that supercharging may have resulted in increased reversibility of interactions between lignin and the CBM. Interestingly, D6 shows the highest percentage of protein recovered amongst all mutants, in stark contrast to D7 and D8, which could partially explain the reason for D6 outperforming its positively supercharged peers (D7 and D8) towards pretreated biomass and cellulose. Lignin inhibition assays were then performed to understand the inhibitory potential of lignin towards hydrolysis of cellulose-I and cellulose-III (see SI Appendix Figure S11 for hydrolysis results and SI Appendix Table T8 for T-tests comparing mutant activities in lignin inhibition assays). Results from lignin inhibition assays were not too instructive due to the high level of error observed in this assay although the overall trends of negatively supercharged mutants outperforming positively supercharged mutants (with the exception of D6) still remained the same.

Overall, the binding assays to cellulose and lignin shed some light on the behavior of D6 as an outliar from the rest of the positively supercharged sub-group, due to increased binding to cellulose-I and reduced irreversible binding to lignin. In addition, D8 shows a dramatic reduction (~ 9-fold) in desorption rate constant towards cellulose-I, indicating that the mutant may struggle with accessing binding sites on cellulose during hydrolysis. However, these results do not explain the reduced activity of D7 toward cellulose-I and AFEX corn stover. It is to be noted that these binding assays are performed at 25 °C as opposed to the hydrolysis assays which are performed at 60 °C. Hence, to understand the potential role of thermal stress on enzyme activity, we subjected these constructs to thermal exposure at elevated temperatures (70 °C), followed by testing of hydrolytic activities at 60 °C.

Hydrolysis of pretreated biomass/cellulose by CBM2a-Cel5A mutants upon thermal treatment: Exposure of the enzymes to 70 °C prior to hydrolysis of AFEX corn stover or cellulose-I revealed differences in thermal stability of the cellulase variants (see Figure 5 for AFEX Corn Stover and Cellulose-I and SI Appendix Figure S12 for EA Corn Stover and Cellulose-III). To quantify this trend, we calculated the percent reduction in activity caused due to thermal treatment which is reported in SI Appendix Table T9. While all enzymes

showed decreased reducing sugar release, D3, D6 and D7 showed the most reduction in activity ($\sim 80-99\%$) towards all substrates tested. On the other hand, D1 and D2 showed better activity upon thermal treatment compared to the wildtype and show the least percent reduction in activity compared to all other mutants.

To build on this trend further, D1, D2 and WT were analyzed further by exposing them to a wider range of temperatures (70 °C, 73 °C, 76 °C and 79 °C) as shown in **Figure 6**. D1 and D2 outshine the wild type especially at higher temperatures such as 76 °C and 79 °C towards AFEX corn stover (see **Figure 6A**) where the wildtype shows practically no activity. For instance, after thermal treatment at 73 °C, D1 and D2 showed ~ 3-fold and ~ 4-fold improvement in activity compared to WT respectively. This difference is even starker at 76 °C although the wild-type activity is closer to the detection limit thereby making activity improvements harder to quantify. However, on cellulose-I (see **Figure 6B**), D1 and D2 showed a steep decrease in activity when the thermal exposure temperature was reduced from 70 °C to 73 °C, which continues to decline at higher temperatures. This may likely be caused by the fact that the reducing sugar release from biomass may be arising from xylan at higher temperatures, which is easily accessible compared to cellulose which requires CBM binding for the catalytic domain to be engaged.

The thermal stability was also measured using a thermal shift assay with SYPRO reagent, and the melting temperatures are reported in **SI Appendix Table T10** (the raw thermal shift assay data is reported in **SI Appendix Figure S13**). There was not an appreciable difference seen in the melting temperatures. This assay measures the melting temperature of the enzyme as a whole and hence these results may be more biased towards the melting temperature of the catalytic domain as opposed to that of the CBM.

Overall, functional hydrolysis assays after thermal treatment of enzymes indicated that supercharging strategy gave rise to thermally stable mutants (D1 and D2) that find direct applications in industry in high-temperature biomass conversion processes. The structural basis of what renders certain supercharged mutants superior to others, still needs to be understood at greater detail which will be the subject of future studies.

CONCLUSIONS

Carbohydrate-binding modules (CBMs) play a crucial role in targeting appended glycoside hydrolase enzymes to plant cell wall polymers such as cellulose and hemicellulose^{63–66}. However, recent studies have shown that CBMs can also play a role in non-productive binding of appended cellulase catalytic domains to cellulose surface^{17,67,68}. In addition, CBMs can bind non-productively to lignin via hydrophobic interactions, leading to deactivation of the enzymes on biomass surface²⁸. To address these bottlenecks, a previous study from our lab has used selective supercharging of cellulase enzymes to reduce lignin inhibition although the mechanistic details were yet to be elucidated²⁹. In this study, we expanded the supercharging

approach to address mechanistic questions surrounding the impact of CBM supercharging on the hydrolysis of real-world pretreated biomass substrates.

This study is the first comprehensive study to test the impact of enzyme supercharging on activity towards various pretreated biomass substrates and systematically deconvolute the interactions of supercharged enzymes with cellulose, xylan and lignin. Although negatively and positively supercharged enzymes showed reduced activity compared to the wild-type, it was identified that some of these mutants show up to 4-fold improved activity upon exposure to higher temperatures. The reduced activity for negatively supercharged mutants was found to be predominantly driven by reduced activity towards xylan, whereas positively supercharged mutants showed reduced activity towards both cellulose and xylan. Future studies should focus on understanding the structural basis of hydrolytic activity and binding of supercharged mutants to lignocellulosic substrates. Recent work has shown that supercharging CBMs may improve catalytic activity on cellulosic biomass due to improved binding, but this outcome may be dependent on supercharging design strategy and the choice of enzymes. ⁶⁹ Moreover, the role of solution pH and salt concentration also need to be studied in greater detail due to their outsized impact on the net charge of the protein and alteration of electrostatic potential of supercharged proteins.

ACKNOWLEDGEMENTS

The authors acknowledge support from the NSF CBET (Award 1604421 and Career Award 1846797), ORAU Ralph E. Powe Award, Rutgers Global Grant, Rutgers Division of Continuing Studies, Rutgers School of Engineering, and the Great Lakes Bioenergy Research Center (DOE BER Office of Science DE-FC02-07ER64494). The authors thank Nathan Kruer-Zerhusen (from late Prof. David Wilson's lab) for kindly providing the *Thermobifida fusca* strain and original Cel5A plasmid DNA. Special thanks to Sarvada Chipkar and Dr. Rebecca Ong at Michigan Technological University, for conducting ammonia pretreatment to provide us with cellulose-III and AFEX corn stover. SPSC would also like to thank Dr. Leonardo Da Sousa (Dale lab at Michigan State University) for conducting ammonia pretreatment to generate cellulose III and EA corn stover that was used here in this study as well. BN would like to thank Patrick Doran (Boston University) for his help initially with setting up protocols for computational protein design using Rosetta. JMY acknowledges support from the Department of Energy, Office of Energy Efficiency and Renewable Energy (EERE) under agreement no. 28598.

SUPPLEMENTARY SECTION

See supplementary information pdf titled 'SI_Appendix.pdf' for supporting results relevant to this study. See pdf document titled 'SI_Appendix_Sequences.pdf', which has the full nucleotide sequences for pEC-CBM2a-Cel5A and pEC-GFP-CBM2a and highlights the mutation sites in CBM2a amino acid sequence.

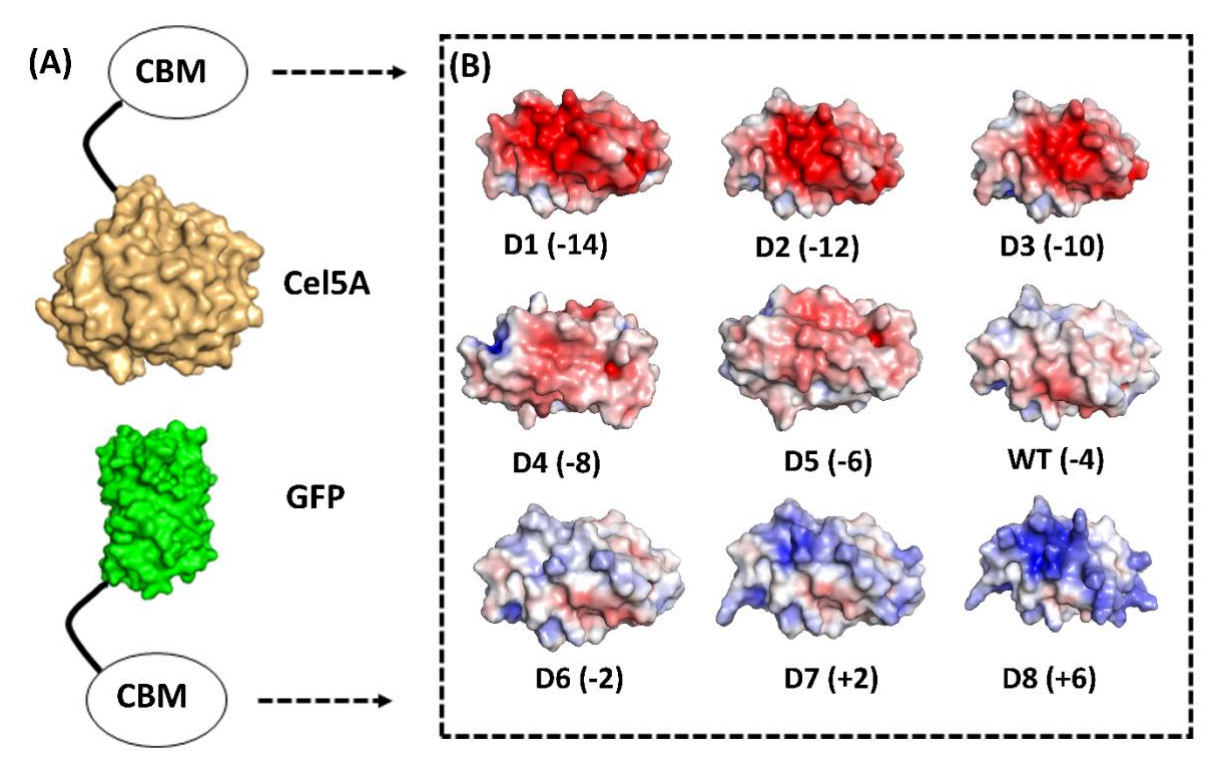


Figure 1. Computational design of supercharged CBM2a mutants and generation of fusion protein constructs. Rosetta was used to identify amino acids on the surface of CBM2a wild-type protein which are amenable to positively charged (K, R) or negatively charged (D, E) amino acid mutations to achieve a target net charge spanning the -14 to +6 range. (A) CBM2a designs were fused with Cel5A and GFP separately. (B) Electrostatic potential maps of the 8 CBM2a designs and their wild-type (represented as WT) are generated using APBS Electrostatics Tool in PyMOL. The name of each construct (D1 – D8 and WT) is followed by the net charge of each design in parenthesis.

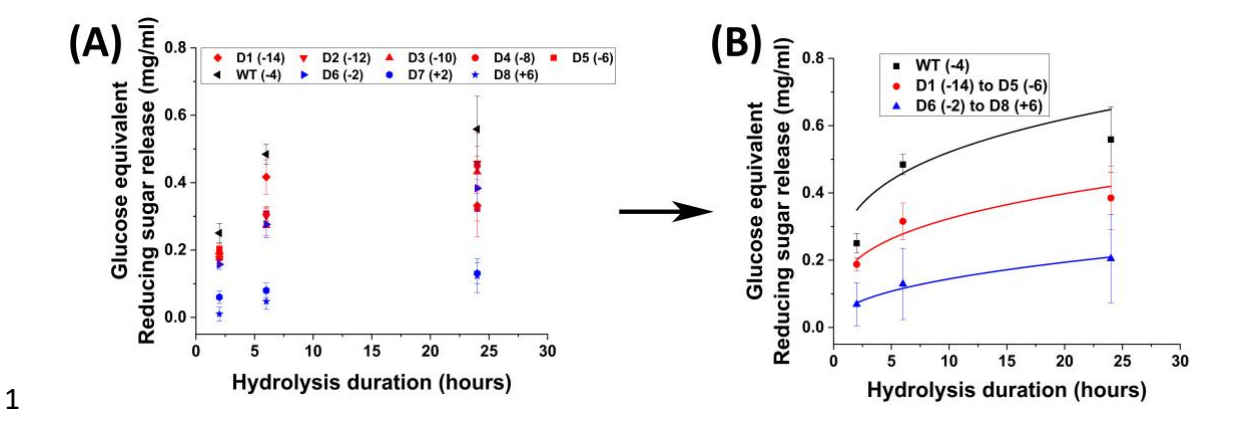


Figure 2. Hydrolytic activity of supercharged cellulases towards AFEX Corn Stover. 80 μL of 25 g/L AFEX Corn Stover was hydrolyzed using an enzyme loading of 120 nmol CBM2a Cel5A fusion enzyme per gram biomass substrate with 12 nmol β-glucosidase enzyme (10% of cellulase loading) per gram biomass substrate for reaction times of 2hrs, 6hrs, and 24hrs. The solubilized reducing sugar concentrations in the supernatant after hydrolysis were determined by the DNS assay (A) Glucose equivalent reducing sugar release (mg/ml) as a function of time (2 hr, 6 hr and 24 hr) for the hydrolysis of AFEX Corn Stover by D1 – D8 CBM2a Cel5A and WT CBM2a Cel5A. Error bars represent standard deviation from the mean, based on at least 4 replicates. (B) Based on the data reported in (A), CBM2a Cel5A fusion constructs with negatively supercharged CBMs (D1 – D5) were grouped together and average hydrolysis yields were obtained for the group, with the error bars representing standard deviation from the mean. Similarly, CBM2a-Cel5A fusion constructs with positively supercharged CBMs (D6 – D8) were grouped together and average hydrolysis yields were obtained. Trend curves have been added to represent the kinetic profiles of the hydrolysis reaction. Wild-type CBM2a-Cel5A is referred to as WT throughout this figure.

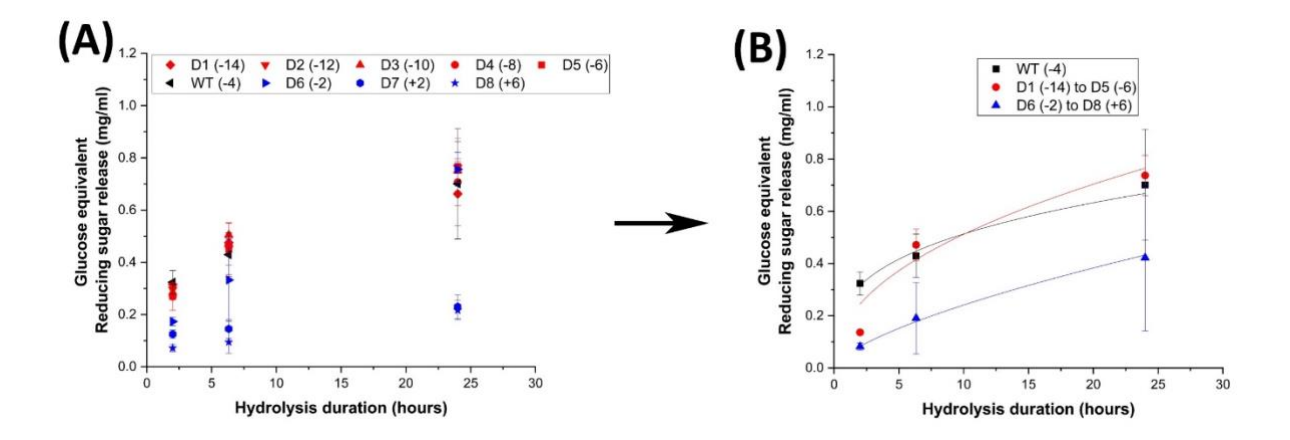


Figure 3: Hydrolytic activity of supercharged cellulases towards Avicel cellulose-I. 40 μL of 100 g/L Avicel cellulose-I substrate was hydrolyzed using an enzyme loading of 120 nmol CBM2a Cel5A fusion enzyme per gram cellulose substrate supplemented with 12 nmol of β-glucosidase enzyme (10% of cellulase loading) per gram cellulose substrate for reaction times of 2hrs, 6hrs, and 24hrs. The solubilized reducing sugar concentrations in the supernatant after hydrolysis were determined by the DNS assay (A) Glucose equivalent reducing sugar release (mg/ml) as a function of time (2 hr, 6 hr and 24 hr) for the hydrolysis of Cellulose-I by D1 – D8 CBM2a Cel5A and WT CBM2a Cel5A. Error bars represent standard deviation from the mean, based on at least 4 replicates. (B) Based on the data reported in (A), CBM2a Cel5A fusion constructs with negatively supercharged CBMs (D1 – D5) were grouped together and average hydrolysis yields were obtained for the group, with the error bars representing standard deviation from the mean. Similarly, CBM2a-Cel5A fusion constructs with positively supercharged CBMs (D6 – D8) were grouped together and average hydrolysis yields were obtained. Trend curves have been added to represent the kinetic profiles of the hydrolysis reaction. Wild-type CBM2a-Cel5A is referred to as WT throughout this figure.

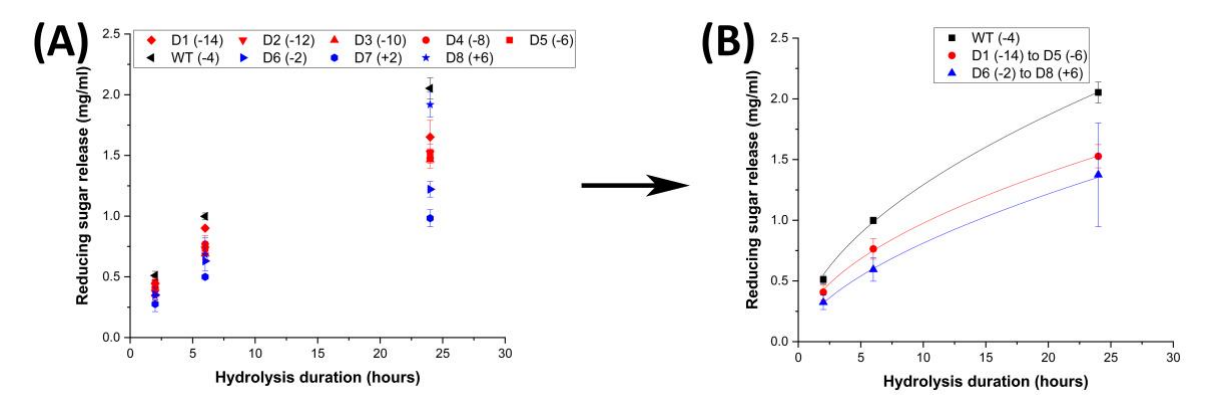


Figure 4: Hydrolytic activity of supercharged cellulases towards Beechwood xylan. 20 μL of 100 g/L Beechwood xylan substrate was hydrolyzed using an enzyme loading of 120 nmol CBM2a Cel5A fusion enzyme per gram xylan substrate supplemented with 12 nmol of β-xylosidase enzyme (10% of cellulase loading) per gram xylan substrate for reaction times of 2hrs, 6hrs, and 24hrs. The solubilized reducing sugar concentrations in the supernatant after hydrolysis were determined by the DNS assay (A) Reducing sugar release (mg/ml) as a function of time (2 hr, 6 hr and 24 hr) for the hydrolysis of Beechwood xylan by D1 – D8 CBM2a Cel5A and WT CBM2a Cel5A. Error bars represent standard deviation from the mean, based on at least 4 replicates. (B) Based on the data reported in (A), CBM2a Cel5A fusion constructs with negatively supercharged CBMs (D1 – D5) were grouped together and average hydrolysis yields were obtained for the group, with the error bars representing standard deviation from the mean. Similarly, CBM2a-Cel5A fusion constructs with positively supercharged CBMs (D6 – D8) were grouped together and average hydrolysis yields were obtained. Trend curves have been added to represent the kinetic profiles of the hydrolysis reaction. Wild-type CBM2a-Cel5A is referred to as WT throughout this figure.

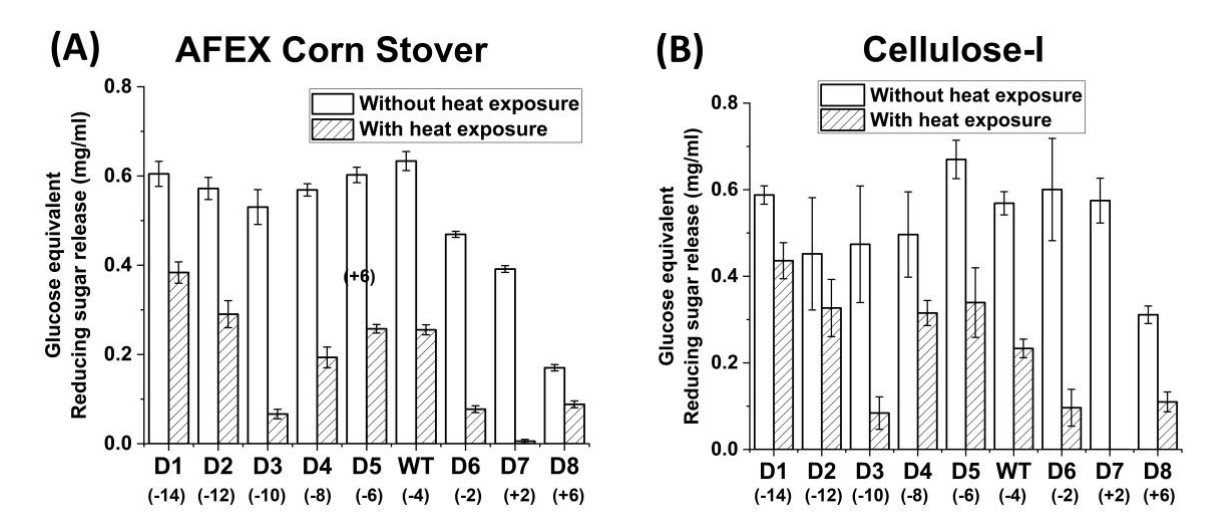


Figure 5. Impact of enzyme thermal denaturation at 70 °C on reducing sugar yields from AFEX corn stover (A) and Avicel cellulose-I (B) Cellulase enzyme (0.0048 nmol/μL concentration) was thermally denatured at 70 °C for 30 minutes using an Eppendorf thermocycler. 50 μl of denatured cellulase enzyme was added to either 80 μl of 25 g/L AFEX Corn Stover (A) or 40 μl of Cellulose-I (B) to establish an effective enzyme loading of 120 nmol enzyme per gram AFEX Corn Stover or Cellulose-I substrate. 12 nmol of β-glucosidase enzyme (10% of cellulase loading) per gram substrate was added to the reaction mixture and incubated at 60 °C for 24 hours. A control reaction was performed with enzyme that was incubated on an ice bath (0 °C) for 30 minutes. The results of enzyme activity upon thermal denaturation at 70 °C are labelled as 'With heat exposure' and those without thermal denaturation are labelled as 'Without heat exposure'. At least 3 replicates were run for each condition and the error bars represent standard deviation from the mean. Reducing sugar yields from hydrolysis of AFEX Corn Stover are reported in (A) and those from Avicel cellulose-I are reported in (B)

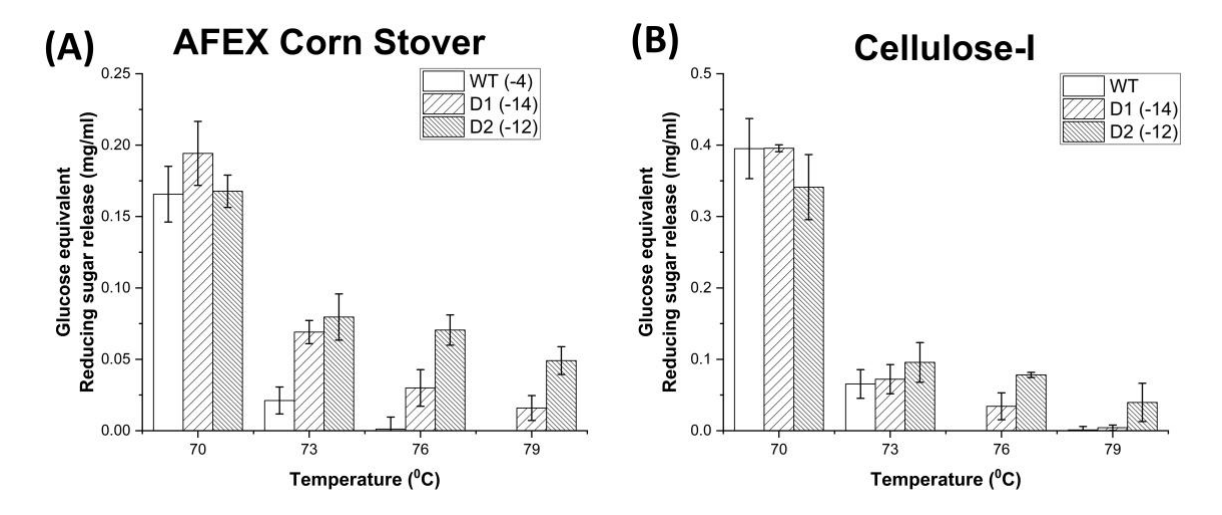


Figure 6: Impact of thermal denaturation at varying temperatures (70 °C, 73 °C, 76 °C and 79 °C) on reducing sugar yields from AFEX Corn Stover (A) and Avicel cellulose-I (B). Cellulase enzyme (0.0048 nmol/μL concentration) was thermally denatured for 30 minutes at one of the following temperatures (70 °C, 73 °C, 76 °C, 79 °C) using an Eppendorf thermocycler. 50 μl of denatured cellulase enzyme was added to either 80 μl of 25 g/L AFEX Corn Stover (A) or 40 μl of Cellulose-I (B) to establish an effective enzyme loading of 120 nmol enzyme per gram AFEX Corn Stover or Cellulose-I substrate. 12 nmol of β-glucosidase enzyme (10% of cellulase loading) per gram substrate was added to the reaction mixture and incubated at 60 °C for 24 hours. A control reaction was performed with enzyme that was incubated on an ice bath (0 °C) for 30 minutes. At least 3 replicates were run for each condition and the error bars represent standard deviation from the mean. Reducing sugar yields from hydrolysis of AFEX Corn Stover are reported in (A) and those from Avicel cellulose-I are reported in (B) under each of the denaturation temperatures (70 °C, 73 °C, 76 °C and 79 °C).

References:

- 2 1. Ubando, A. T., Felix, C. B. & Chen, W. H. Biorefineries in circular bioeconomy: A
- 3 comprehensive review. *Bioresource Technology* **299**, (2020).
- 4 2. Tuck, C. O., Perez, E., Horvath, I. T., Sheldon, R. A. & Poliakoff, M. Valorization of
- 5 Biomass: Deriving More Value from Waste. Science (80-.). 338, 604 (2012).
- 6 3. Chundawat, S. P. S., Beckham, G. T., Himmel, M. E. & Dale, B. E. Deconstruction of
- 7 Lignocellulosic Biomass to Fuels and Chemicals. **2**, 121–145 (2011).
- 8 4. Kokossis, A. C., Tsakalova, M. & Pyrgakis, K. Design of integrated biorefineries.
- 9 *Comput. Chem. Eng.* **81**, 40–56 (2014).
- 10 5. Maity, S. K. Opportunities, recent trends and challenges of integrated biorefinery: Part
- i. Renew. Sustain. Energy Rev. 43, 1427–1445 (2015).
- Wang, H., Pu, Y., Ragauskas, A. & Yang, B. From lignin to valuable products—
- strategies, challenges, and prospects. *Bioresour. Technol.* **271**, 449–461 (2019).
- 14 7. Ragauskas, A. J. et al. Lignin valorization: Improving lignin processing in the
- biorefinery. *Science* (80-.). **344**, (2014).
- 16 8. Takkellapati, S., Li, T. & Gonzalez, M. A. An overview of biorefinery-derived
- platform chemicals from a cellulose and hemicellulose biorefinery. *Clean Technol*.
- 18 Environ. Policy **20**, 1615–1630 (2018).
- 9. Scown, C. D., Baral, N. R., Yang, M., Vora, N. & Huntington, T. Technoeconomic
- analysis for biofuels and bioproducts. *Curr. Opin. Biotechnol.* **67**, 58–64 (2021).
- 21 10. Humbird, D. et al. Process Design and Economics for Biochemical Conversion of
- 22 Lignocellulosic Biomass to Ethanol: Dilute-Acid Pretreatment and Enzymatic
- 23 Hydrolysis of Corn Stover. in *NREL/TP-5100-47764* (National Renewable Energy
- Laboratory, Golden, CO, USA, 2011).
- 25 11. Klein-Marcuschamer, D., Oleskowicz-Popiel, P., Simmons, B. A. & Blanch, H. W.
- The challenge of enzyme cost in the production of lignocellulosic biofuels. *Biotechnol*.
- 27 Bioeng. 109, (2012).
- 28 12. McCann, M. C. & Carpita, N. C. Biomass recalcitrance: A multi-scale, multi-factor,
- and conversion-specific property. *Journal of Experimental Botany* **66**, (2015).
- 30 13. Holwerda, E. K. et al. Multiple levers for overcoming the recalcitrance of
- 31 lignocellulosic biomass. *Biotechnol. Biofuels* **12**, 1–12 (2019).
- 32 14. Zeng, Y., Zhao, S., Yang, S. & Ding, S. Y. Lignin plays a negative role in the
- biochemical process for producing lignocellulosic biofuels. Current Opinion in
- 34 *Biotechnology* **27**, (2014).
- 35 15. Studer, M. H. et al. Lignin content in natural populus variants affects sugar release.
- 36 *Proc. Natl. Acad. Sci. U. S. A.* **108**, 6300–6305 (2011).
- 37 16. Strobel, K. L., Pfeiffer, K. A., Blanch, H. W. & Clark, D. S. Structural insights into the
- affinity of Cel7A carbohydratebinding module for lignin. J. Biol. Chem. 290, 22818–
- 39 22826 (2015).
- 40 17. Nemmaru, B. et al. Reduced type-A carbohydrate-binding module interactions to
- 41 cellulose I leads to improved endocellulase activity. *Biotechnol. Bioeng.* **118**, (2021).
- 42 18. Narron, R. H., Kim, H., Chang, H. M., Jameel, H. & Park, S. Biomass pretreatments

- capable of enabling lignin valorization in a biorefinery process. *Curr. Opin.*
- 2 Biotechnol. 38, 39–46 (2016).
- 3 19. Galbe, M. & Wallberg, O. Pretreatment for biorefineries: A review of common
- 4 methods for efficient utilisation of lignocellulosic materials. *Biotechnology for*
- 5 *Biofuels* **12**, (2019).
- 6 20. Chen, X. et al. DMR (deacetylation and mechanical refining) processing of corn stover
- 7 achieves high monomeric sugar concentrations (230 g L-1) during enzymatic
- 8 hydrolysis and high ethanol concentrations (>10% v/v) during fermentation without
- 9 hydrolysate purification or c. *Energy Environ. Sci.* **9**, 1237–1245 (2016).
- 10 21. Chundawat, S. P. S. et al. Multi-scale visualization and characterization of
- lignocellulosic plant cell wall deconstruction during thermochemical pretreatment † ‡.
- doi:10.1039/c0ee00574f
- 13 22. Salas, C., Rojas, O. J., Lucia, L. a, Hubbe, M. a & Genzer, J. On the surface
- interactions of proteins with lignin. ACS Appl. Mater. Interfaces 5, 199–206 (2013).
- 15 23. Guo, F. et al. Differences in the adsorption of enzymes onto lignins from diverse types
- of lignocellulosic biomass and the underlying mechanism. *Biotechnol. Biofuels* **7**, 1–10
- 17 (2014).
- 18 24. Sammond, D. W. et al. Predicting enzyme adsorption to lignin films by calculating
- 19 enzyme surface hydrophobicity. *J. Biol. Chem.* **289**, 20960–20969 (2014).
- 20 25. Yang, B. & Wyman, C. E. BSA treatment to enhance enzymatic hydrolysis of
- cellulose in lignin containing substrates. *Biotechnol. Bioeng.* **94**, 611–617 (2006).
- 22 26. Luo, X. et al. Promoting enzymatic hydrolysis of lignocellulosic biomass by
- inexpensive soy protein. *Biotechnol. Biofuels* **12**, 1–13 (2019).
- 24 27. Nordwald, E. M., Brunecky, R., Himmel, M. E., Beckham, G. T. & Kaar, J. L. Charge
- engineering of cellulases improves ionic liquid tolerance and reduces lignin inhibition.
- 26 *Biotechnol. Bioeng.* **111**, 1541–1549 (2014).
- 27 28. Haarmeyer, C. N., Smith, M. D., Chundawat, S. P. S., Sammond, D. & Whitehead, T.
- A. Insights into cellulase-lignin non-specific binding revealed by computational
- redesign of the surface of green fluorescent protein. *Biotechnol. Bioeng.* **114**, 740–750
- 30 (2017).
- 31 29. Whitehead, T. A., Bandi, C. K., Berger, M., Park, J. & Chundawat, S. P. S. Negatively
- 32 Supercharging Cellulases Render Them Lignin-Resistant. ACS Sustain. Chem. Eng. 5,
- 33 (2017).
- 34 30. Der, B. S. et al. Alternative Computational Protocols for Supercharging Protein
- Surfaces for Reversible Unfolding and Retention of Stability. *PLoS One* **8**, (2013).
- 36 31. Lawrence, M. S., Phillips, K. J. & Liu, D. R. Supercharging proteins can impart
- 37 unusual resilience. J. Am. Chem. Soc. **129**, 10110–10112 (2007).
- 38 32. Thompson, D. B., Cronican, J. J. & Liu, D. R. Engineering and Identifying
- 39 Supercharged Proteins for Macromolecule Delivery into Mammalian Cells. *Methods*
- 40 Enzymol. **1067**, 293–319 (2012).
- 41 33. Lei, C. et al. A supercharged fluorescent protein as a versatile probe for homogeneous
- DNA detection and methylation analysis. *Angew. Chemie Int. Ed.* **53**, 8358–8362

- 1 (2014).
- 2 34. Obermeyer, A. C., Mills, C. E., Dong, X. H., Flores, R. J. & Olsen, B. D. Complex
- 3 coacervation of supercharged proteins with polyelectrolytes. *Soft Matter* **12**, 3570–
- 4 3581 (2016).
- 5 35. Simon, A. J. et al. Supercharging enables organized assembly of synthetic
- 6 biomolecules. *Nat. Chem.* **11**, 204–212 (2019).
- 7 36. Sasaki, E. et al. Structure and assembly of scalable porous protein cages. Nat.
- 8 *Commun.* **8**, 1–10 (2017).
- 9 37. Beck, T., Tetter, S., Künzle, M. & Hilvert, D. Construction of Matryoshka-Type
- Structures from Supercharged Protein Nanocages. *Angew. Chemie* **127**, 951–954
- **11** (2015).
- 12 38. Azuma, Y., Zschoche, R., Tinzl, M. & Hilvert, D. Quantitative Packaging of Active
- Enzymes into a Protein Cage. Angew. Chemie Int. Ed. 55, 1531–1534 (2016).
- 14 39. Alford, R. F. et al. The Rosetta All-Atom Energy Function for Macromolecular
- 15 Modeling and Design. *J. Chem. Theory Comput.* **13**, 3031–3048 (2017).
- 16 40. Das, R. & Baker, D. Macromolecular modeling with Rosetta. *Annu. Rev. Biochem.* 77,
- 17 363–382 (2008).
- 18 41. Kleffner, R. et al. Foldit Standalone: a video game-derived protein structure
- manipulation interface using Rosetta. *Bioinformatics* **33**, 2765–2767 (2017).
- 20 42. Liu, Y., Nemmaru, B. & Chundawat, S. P. S. Thermobifida fusca Cellulases Exhibit
- 21 Increased Endo Exo Synergistic Activity, but Lower Exocellulase Activity, on
- 22 Cellulose-III. ACS Sustain. Chem. Eng. 8, 5028–5039 (2020).
- 23 43. Wilson, D. B. Studies of Thermobifida fusca plant cell wall degrading enzymes. *Chem.*
- 24 *Rec.* **4**, (2004).
- 25 44. Chundawat, S. P. S. et al. Ammonia-salt solvent promotes cellulosic biomass
- deconstruction under ambient pretreatment conditions to enable rapid soluble sugar
- production at ultra-low enzyme loadings. *Green Chem.* **22**, 204–218 (2020).
- 28 45. Da Costa Sousa, L. et al. Next-generation ammonia pretreatment enhances cellulosic
- biofuel production. *Energy Environ. Sci.* **9**, (2016).
- 30 46. Sousa, L. da C., Humpula, J., Balan, V., Dale, B. E. & Chundawat, S. P. S. Impact of
- 31 Ammonia Pretreatment Conditions on the Cellulose III Allomorph Ultrastructure and
- 32 Its Enzymatic Digestibility. ACS Sustain. Chem. Eng. 7, 14411–14424 (2019).
- 33 47. Chundawat, S. P. S. et al. Restructuring the crystalline cellulose hydrogen bond
- network enhances its depolymerization rate. J. Am. Chem. Soc. 133, 11163–11174
- 35 (2011).
- 36 48. Bozell, J. J. et al. Solvent fractionation of renewable woody feedstocks: Organosolv
- generation of biorefinery process streams for the production of biobased chemicals.
- 38 *Biomass and Bioenergy* **35**, 4197–4208 (2011).
- 39 49. Song, Y. et al. High-resolution comparative modeling with RosettaCM. Structure 21,
- 40 1735–1742 (2013).
- 41 50. Burley, S. K. et al. RCSB Protein Data Bank: Powerful new tools for exploring 3D
- structures of biological macromolecules for basic and applied research and education

- in fundamental biology, biomedicine, biotechnology, bioengineering and energy sciences. *Nucleic Acids Res.* **49**, D437–D451 (2021).
- 3 51. Khatib, F. *et al.* Algorithm discovery by protein folding game players. *Proc. Natl.*
- 4 Acad. Sci. U. S. A. 108, (2011).
- 5 52. Watson, D. L., Wilson, D. B. & Walker, L. P. Synergism in binary mixtures of
- 6 Thermobifida fusca cellulases Cel6b, Cel9a, and Cel5a on BMCC and Avicel. *Appl.*
- 7 Biochem. Biotechnol. Part A Enzym. Eng. Biotechnol. 101, 97–111 (2002).
- 8 53. Jung, H., Wilson, D. B. & Walker, L. P. Binding and reversibility of Thermobifida
- 9 fusca Cel5A, Cel6B, and Cel48A and their respective catalytic domains to bacterial
- microcrystalline cellulose. *Biotechnol. Bioeng.* **84**, 151–159 (2003).
- 11 54. Blommel, P. G., Martin, P. A., Seder, K. D., Wrobel, R. L. & Fox, B. G. Flexi Vector
- 12 Cloning. in High Throughput Protein Expression and Purification: Methods and
- 13 *Protocols* (ed. Doyle, S. A.) 55–73 (Humana Press, 2009). doi:10.1007/978-1-59745-
- 14 196-3 4
- 15 55. Lim, S., Chundawat, S. P. S. & Fox, B. G. Expression, Purification and
- 16 Characterization of a Functional Carbohydrate-Binding Module from Streptomyces sp.
- 17 SirexAA-E. *Protein Expr. Purif.* **98**, 1–9 (2014).
- 18 56. Studier, F. W. Protein production by auto-induction in high-density shaking cultures.
- 19 *Protein Expr. Purif.* **41**, 207–234 (2005).
- 20 57. Kostylev, M. & Wilson, D. Two-parameter kinetic model based on a time-dependent
- 21 activity coefficient accurately describes enzymatic cellulose digestion. *Biochemistry*
- **52**, 5656–5664 (2013).
- 23 58. Brunecky, R. et al. Synthetic fungal multifunctional cellulases for enhanced biomass
- 24 conversion. *Green Chem.* **22**, 478–489 (2020).
- 25 59. Gao, D. et al. Lignin triggers irreversible cellulase loss during pretreated
- lignocellulosic biomass saccharification. *Biotechnol. Biofuels* 7, 175 (2014).
- 27 60. Sun, C., Li, Y., Yates, E. A. & Fernig, D. G. SimpleDSFviewer: A tool to analyze and
- view differential scanning fluorimetry data for characterizing protein thermal stability
- and interactions. *Protein Sci.* **29**, 19–27 (2020).
- 30 61. Georgelis, N., Yennawar, N. H. & Cosgrove, D. J. Structural basis for entropy-driven
- 31 cellulose binding by a type-A cellulose-binding module (CBM) and bacterial expansin.
- 32 *Proc. Natl. Acad. Sci. U. S. A.* **109**, 14830–14835 (2012).
- 33 62. Nimlos, M. R. et al. Binding preferences, surface attachment, diffusivity, and
- orientation of a family 1 carbohydrate-binding module on cellulose. *J. Biol. Chem.*
- 35 (2012). doi:10.1074/jbc.M112.358184
- 36 63. McLean, B. W. et al. Carbohydrate-binding modules recognize fine substructures of
- 37 cellulose. *J. Biol. Chem.* **277**, 50245–50254 (2002).
- 38 64. Herve, C. et al. Carbohydrate-binding modules promote the enzymatic deconstruction
- of intact plant cell walls by targeting and proximity effects. *Proc. Natl. Acad. Sci.* **107**,
- 40 15293–15298 (2010).
- 41 65. Reyes-Ortiz, V. et al. Addition of a carbohydrate-binding module enhances cellulase
- penetration into cellulose substrates. *Biotechnol. Biofuels* **6**, (2013).

- Fox, J. M. *et al.* A single-molecule analysis reveals morphological targets for cellulase synergy. *Nat. Chem. Biol.* **9**, 356–361 (2013).
- Karuna, N. & Jeoh, T. The productive cellulase binding capacity of cellulosic
 substrates. *Biotechnol. Bioeng.* (2017). doi:10.1002/bit.26193
- Nill, J. & Jeoh, T. The role of evolving interfacial substrate properties on
 heterogeneous cellulose hydrolysis kinetics. *ACS Sustain. Chem. Eng.* 8, 6722–6733
 (2020).
- DeChellis, A. *et al.* Supercharging Carbohydrate Binding Module Alone Enhances
 Endocellulase Thermostability, Binding, and Activity on Cellulosic Biomass. *ACS Sustain. Chem. Eng.* 12, (2024).

Supplementary Information (SI) Document

Supercharged cellulases show superior thermal stability and enhanced activity towards pretreated biomass and cellulose

Bhargava Nemmaru^{a,#}, Jenna Douglass^{a,#}, John M Yarbrough^b, Antonio De Chellis^a, Srivatsan Shankar^a, Alina Thokkadam^a, Allan Wang^a, Shishir P. S. Chundawat^{a,1}

Corresponding Author Name: Shishir P. S. Chundawat* (ORCID: 0000-0003-3677-6735)

Corresponding Author Email: shishir.chundawat@rutgers.edu

Number of SI pages in current PDF (SI-Supplementary Information): 25

Number of SI figures in current PDF (SI-Supplementary Information): 13

Number of SI tables in current PDF (SI-Supplementary Information): 11

Number of SI files (including current PDF): 2

^a Department of Chemical & Biochemical Engineering, Rutgers The State University of New Jersey, Piscataway, New Jersey 08854, USA.

^b Biosciences Center, National Renewable Energy Lab, Golden, Colorado 80401, USA.

[#] Equal contribution

¹Corresponding Author: Shishir P. S. Chundawat (<u>shishir.chundawat@rutgers.edu</u>, Tel: 848-445-3678)

	Mutation to K	Mutation to R	Mutation to D	Mutation to E	Average mutation energy score (K, R, D, E)
		Clus	ter 1		
N39	0.972	1.339	-1.545	-0.372	0.0985
T51	-0.319	-1.632	0.507	-0.391	-0.45875
Q55	-0.964	-0.648	-0.185	-0.308	-0.52625
S81	-0.804	-0.173	0.159	-1.979	-0.69925
S53	-1.236	-0.886	-1.314	-0.818	-1.0635
S83	-0.263	1.587	-0.859	-0.386	0.01975
		Clus	ter 2		
T49	-0.925	-1.243	0.01	-0.628	-0.6965
T31	-1.96	-1.625	0.246	0.362	-0.74425
S25	-0.503	-1.424	-1.112	-0.31	-0.83725
S60	-0.925	-0.707	-1.133	-1.008	-0.94325
N28	-1.944	-1.806	-0.413	-2.676	-1.70975

Table T1: Rosetta mutation energy scores for polar uncharged surface residues based after multiple fast relax operations until the energy score equilibrates. K, R, D, E mutations were scored for each polar uncharged residue using Rosetta and an average mutation energy score was obtained. Based on the homology model of wild-type CBM2a, these residues were organized into two spatially distinct clusters.

Design	Net Charge	Mutations
D1	-14	N39D, T49E, T51E, T31D, Q55E, S25D, S81E, S60E, S53D, N28E
D2	-12	N39D, T49E, T51E, T31D, Q55E, S25D, S81E, S60E
D3	-10	N39D, T49E, T51E, T31D, Q55E, S25D
D4	-8	N39D, T49E, T51E, T31D
D5	-6	N39D, T49E
D6	-2	T51K, T31K
D7	+2	T51K, T31K, Q55K, S25R, S81K, S60K
D8	+6	T51K, T31K, Q55K, S25R, S81K, S60K, S53K, N28K, N39K, T49R

Table T2: Mutations on wild-type CBM2a to generate supercharged mutant designs. Based on the average energy scores computed in previous table T1, surface residues were either mutated to a negatively charged residue (D, E) or a positively charged residue (R, K) to obtain a target net charge. This table reports the list of mutations necessary to generate a certain CBM2a mutant design (D1-D8) from CBM2a wild-type.

		AFEX Corn Stover		EA	ver			
Construct 1	Construct 2	2 hrs	6 hrs	24 hrs	2 hrs	6 hrs	24 hrs	
Co	Comparison between negatively supercharged constructs (D1 - D5)							
D1	D2	0.232	0.044	0.062	0.728	0.001	0.040	
D1	D3	0.210	0.021	0.015	0.839	0.002	0.036	
D1	D4	0.736	0.053	0.007	0.645	0.001	0.356	
D1	D5	0.152	0.055	0.546	0.154	0.005	0.710	
D2	D3	0.776	0.093	0.684	0.337	0.129	0.713	
D2	D4	0.201	0.512	0.907	0.827	0.765	0.015	
D2	D5	0.041	0.343	0.110	0.050	0.734	0.029	
D3	D4	0.222	0.060	0.657	0.386	0.406	0.012	
D3	D5	0.011	0.045	0.086	0.008	0.215	0.038	
D4	D5	0.398	0.607	0.054	0.214	0.597	0.172	
C	Comparison between positively supercharged constructs (D6 - D8)							
D6	D7	0.000	0.008	0.015	0.000	0.000	0.000	
D7	D8	0.004	0.026	0.834	0.003	0.000	0.012	
D6	D8	0.000	0.003	0.008	0.000	0.000	0.000	

Table T3: p-values from Student's T-test for comparison of biomass hydrolysis yields from CBM2a-Cel5A fusion constructs. Student's T-test was conducted to compare biomass hydrolysis yields of every pair in the negatively charged group (D1 – D6) and every pair in the positively charged group (D7 – D8). The raw data is reported in Figure 2 of the main manuscript and Figure S5 of the SI Appendix

	AFEX Corn Stover			EA Corn Stover		
Enzyme Design	A	b	Adjusted R- Square	A	b	Adjusted R- Square
D1 (-14)	0.35 ± 0.32	0.02 ± 0.34	0.99	0.37 ± 0.13	0.25 ± 0.13	0.99
D2 (-12)	0.15 ± 0.02	0.37 ± 0.07	1.00	0.21 ± 0.04	0.39 ± 0.06	1.00
D3 (-10)	0.14 ± 0.00	0.35 ± 0.01	1.00	0.19 ± 0.03	0.42 ± 0.05	1.00
D4 (-8)	0.17 ± 0.01	0.32 ± 0.05	1.00	0.17 ± 0.02	0.50 ± 0.03	1.00
D5 (-6)	0.19 ± 0.05	0.23 ± 0.13	1.00	0.20 ± 0.02	0.44 ± 0.04	1.00
WT (-4)	0.29 ± 0.12	0.25 ± 0.18	1.00	0.30 ± 0.09	0.42 ± 0.10	0.99
D6 (-2)	0.14 ± 0.03	0.35 ± 0.08	0.99	0.27 ± 0.08	0.30 ± 0.12	1.00
D7 (+2)	0.047 ± 0.00	0.32 ± 0.03	0.99	0.14 ± 0.06	0.28 ± 0.16	1.00
D8 (+6)	0.009 ± 0.004	0.81 ± 0.16	0.99	0.049 ± 0.027	0.51 ± 0.24	1.00
D1-D5	0.16 ± 0.03	0.30 ± 0.10	0.99	0.19 ± 0.00	0.45 ± 0.00	0.99
D6-D8	0.05 ± 0.00	0.43 ± 0.06	0.99	0.09 ± 0.00	0.50 ± 0.00	0.99

Table T4: Kinetic parameter fits for biomass hydrolysis by CBM2a-Cel5A fusion constructs. Reaction progress curves for hydrolysis of AFEX and EA pretreated corn stover (reported in **Figure 2** of the main manuscript and **Figure S5** of the SI Appendix) by CBM2a-Cel5A fusion constructs was fit to a power curve represented by the formula $Percent\ conversion = A * time^b$. Curve fitting was done in Origin and the averages, standard errors from mean for each parameter are reported here. WT refers to wild-type.

		Cellulose-I			Cellulose-III			
Construct 1	Construct 2	2 hrs	6 hrs	24 hrs	2 hrs	6 hrs	24 hrs	
Co	Comparison between negatively supercharged constructs (D1 – D5)							
D1	D2	0.158	0.716	0.152	0.385	0.162	0.382	
D1	D3	0.881	0.129	0.603	0.213	0.173	0.449	
D1	D4	0.264	0.697	0.770	0.147	0.158	0.094	
D1	D5	0.014	0.610	0.201	0.150	0.157	0.306	
D2	D3	0.507	0.437	0.729	0.049	0.045	0.065	
D2	D4	0.467	0.813	0.719	0.560	0.090	0.143	
D2	D5	0.074	0.975	0.947	0.625	0.690	0.258	
D3	D4	0.653	0.171	0.770	0.854	0.062	0.226	
D3	D5	0.319	0.344	0.819	0.939	0.066	0.874	
D4	D5	0.983	0.721	0.705	0.828	0.015	0.153	
Co	Comparison between positively supercharged constructs (D6 - D8)							
D6	D7	0.065	0.334	0.002	0.309	0.005	0.039	
D7	D8	0.010	0.196	0.760	0.000	0.001	0.149	
D6	D8	0.018	0.266	0.001	0.095	0.004	0.000	

Table T5: p-values from Student's T-test for comparison of crystalline cellulose hydrolysis yields from CBM2a-Cel5A fusion constructs. Student's T-test was conducted to compare biomass hydrolysis yields of every pair in the negatively charged group (D1 - D6) and every pair in the positively charged group (D7 - D8). The raw data for Cellulose-I and Cellulose_III are reported in **Figure 3** of the main manuscript and **Figure S7** of the SI Appendix respectively.

		Cellulose-I		Cellulose-III		
Enzyme Design	A	b	Adjusted R- Square	A	b	Adjusted R- Square
D1 (-14)	0.27 ± 0.02	0.28 ± 0.03	1.00	0.24 ± 0.06	0.59 ± 0.08	1.00
D2 (-12)	0.23 ± 0.00	0.38 ± 0.00	1.00	0.17 ± 0.04	0.73 ± 0.08	1.00
D3 (-10)	0.25 ± 0.04	0.35 ± 0.05	1.00	0.26 ± 0.01	0.60 ± 0.02	1.00
D4 (-8)	0.23 ± 0.03	0.38 ± 0.07	1.00	0.34 ± 0.06	0.54 ± 0.06	1.00
D5 (-6)	0.21 ± 0.01	0.42 ± 0.01	1.00	0.18 ± 0.04	0.71 ± 0.07	1.00
WT (-4)	0.26 ± 0.02	0.30 ± 0.04	1.00	0.22 ± 0.07	0.57 ± 0.11	1.00
D6 (-2)	0.11 ± 0.00	0.60 ± 0.01	1.00	0.28 ± 0.05	0.58 ± 0.06	1.00
D7 (+2)	0.10 ± 0.01	0.24 ± 0.05	0.96	0.10 ± 0.09	0.57 ± 0.51	1.00
D8 (+6)	0.05 ± 0.01	0.46 ± 0.07	0.99	0.04 ± 0.02	0.56 ± 0.21	1.00
D1-D5	0.18 ± 0.11	0.46 ± 0.21	1.00	0.22 ± 0.01	0.64 ± 0.01	0.99
D6-D8	0.05 ± 0.00	0.67 ± 0.03	1.00	0.15 ± 0.00	0.58 ± 0.01	1.00

Table T6: Kinetic parameter fits for crystalline cellulose hydrolysis by CBM2a-Cel5A fusion constructs. Reaction progress curves for hydrolysis of cellulose-I and cellulose-III (reported in Figure 3 of the main manuscript Figure S7 of the SI Appendix) by CBM2a-Cel5A fusion constructs was fit to a power curve represented by the formula $Percent conversion = A * time^b$. Curve fitting was done in Origin and the averages, standard errors from mean for each parameter are reported here. WT refers to wild type.

	Binding to Lignin						
CBM2a Design	Number of binding sites (* 10 ¹² molecules)	Percent protein recovered					
D1 (-14)	23.46 ± 0.31	34.41 ± 2.84					
D2 (-12)	25.42 ± 3.17	25.44 ± 0.27					
D3 (-10)	18.83 ± 4.41	44.09 ± 16.16					
D4 (-8)	26.11 ± 2.55	32.35 ± 5.54					
D5 (-6)	41.05 ± 4.24	38.70 ± 1.41					
WT (-4)	33.18 ± 1.02	19.55 ± 1.92					
D6 (-2)	30.44 ± 2.18	49.22 ± 3.25					
D7 (+2)	35.63 ± 2.43	31.52 ± 9.10					
D8 (+6)	37.24 ± 1.75	32.18 ± 0.00					

Table T7: Binding of GFP-CBM2a fusion proteins to lignin. Quartz crystal microbalance with dissipation (QCM-D) was used to study the binding of GFP-CBM2a designs to crystalline lignin. Number of binding sites (* 10¹² molecules) and percent protein recovered was computed for lignin since binding was observed to be mostly irreversible. Experiments were performed in 2 replicates and the average along with standard deviation computed for these measurements which is reported here.

	Cellu	lose-I	Cellulose-III		
	Comparison to D7 Comparison		Comparison to D7	Comparison to D8	
D 1	0.001	0.002	0.003	0.006	
D2	0.002	0.003	0.000	0.001	
D3	0.000	0.001	0.003	0.006	
D4	0.022	0.031	0.017	0.040	
D5	0.000	0.001	0.000	0.000	
D6	0.028	0.040	0.083	0.413	
WT	0.001	0.001	0.004	0.010	

Table T8: p-values from Student's T-test for comparison of hydrolysis yields in the presence of lignin. Student's T-test was conducted to compare the hydrolysis yields of all the constructs in negatively charged group (D1 - D6) to all the constructs in positively charged group (D7 - D8). These results reveal statistically significant differences between any pair of constructs where one mutant construct is derived from the positively charged group

Mutant	AFEX Corn Stover	Cellulose-I	EA Corn Stover	Cellulose-III
D1 (-14)	36.6	25.8	30.0	39.7
D2 (-12)	49.2	27.7	50.4	55.3
D3 (-10)	87.4	82.3	87.5	91.9
D4 (-8)	66.0	36.5	70.0	60.4
D5 (-6)	57.2	49.3	61.6	59.5
WT (-4)	59.7	59.0	61.0	57.7
D6 (-2)	83.5	83.9	84.3	89.1
D7 (+2)	98.6	101.0	98.6	99.8
D8 (+6)	48.2	64.7	57.4	77.7

Table T9: **Percent reduction in hydrolytic activity upon thermal denaturation at 70** °C Based on results reported in Figure 5 (for AFEX Corn Stover and Cellulose-I) and SI Figure S11 (for EA Corn Stover and Cellulose-III), percentage reduction in hydrolytic activity between non-thermally treated enzyme and thermally treated enzyme on each substrate.

Design	Net charge	T _m (°C)
D1	-14	73.74 ± 0.08
D2	-12	73.36 ± 0.11
D3	-10	73.62 ± 0.15
D4	-8	74.84 ± 0.03
D5	-6	74.32 ± 0.12
WT	-4	74.02 ± 0.01
D6	-2	73.54 ± 0.17
D7	+2	73.67 ± 0.07
D8	+6	74.22 ± 0.11

Table T10. Melting temperatures of CBM2a-Cel5A measured via thermal shift assays. Thermal shift assays were conducted using 5 μ l 200X SYPRO reagent, 5 μ l 0.5 M sodium acetate buffer (pH 5.5), 5 μ M enzyme dilution and deionized water to make up to 50 μ l. The mixtures were exposed to a temperature ramp from 25 °C to 99 °C at a rate of 0.04 °C per second using QuantStudio 3 real-time PCR equipment and fluorescence measured (excitation – 470 nm; emission – 520 nm). Melting temperatures (T_m) were obtained from each individual trace and averages with standard deviations reported here.

Design	Molecular Weight (kDa)	Enzyme Loading (mg enzyme per gram biomass)
D1	48.202	5.784
D2	48.244	5.789
D3	48.273	5.793
D4	48.357	5.803
D5	48.517	5.822
WT	48.173	5.781
D6	48.227	5.787
D7	48.378	5.805
D8	48.503	5.820

Table T11. Hydrolysis assay enzyme loading on a mass basis. Molecular weights for the entire supercharged CBM2a – Cel5A library were obtained using Geneious bioinformatic software. Enzyme loadings are reported here as mg of enzyme per gram of biomass converted from the standard 120 nmol enzyme per gram of biomass loading used in all hydrolysis assays in the study.

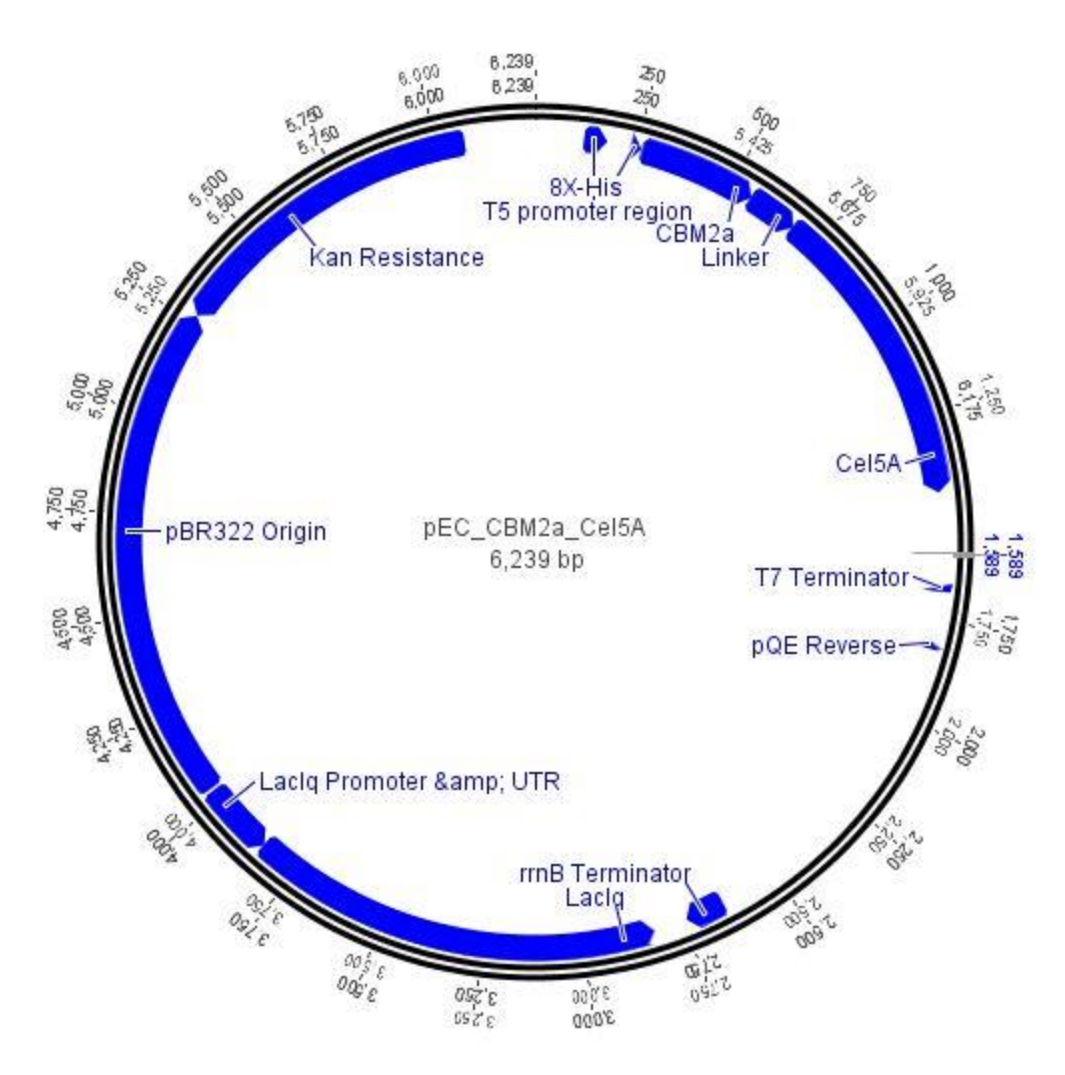


Figure S1: Plasmid map for pEC-CBM2a-Cel5A Open reading frame consisting of 8X Histidine tag (labeled 8X-His) followed by CBM2a wild-type, linker and Cel5A is highlighted. pEC plasmid backbone consists of T5 promoter region and T7 terminator region as described elsewhere¹. Other elements highlighted here are: pBR322 origin of replication, LacI promoter and gene to enable lactose-inducible expression.

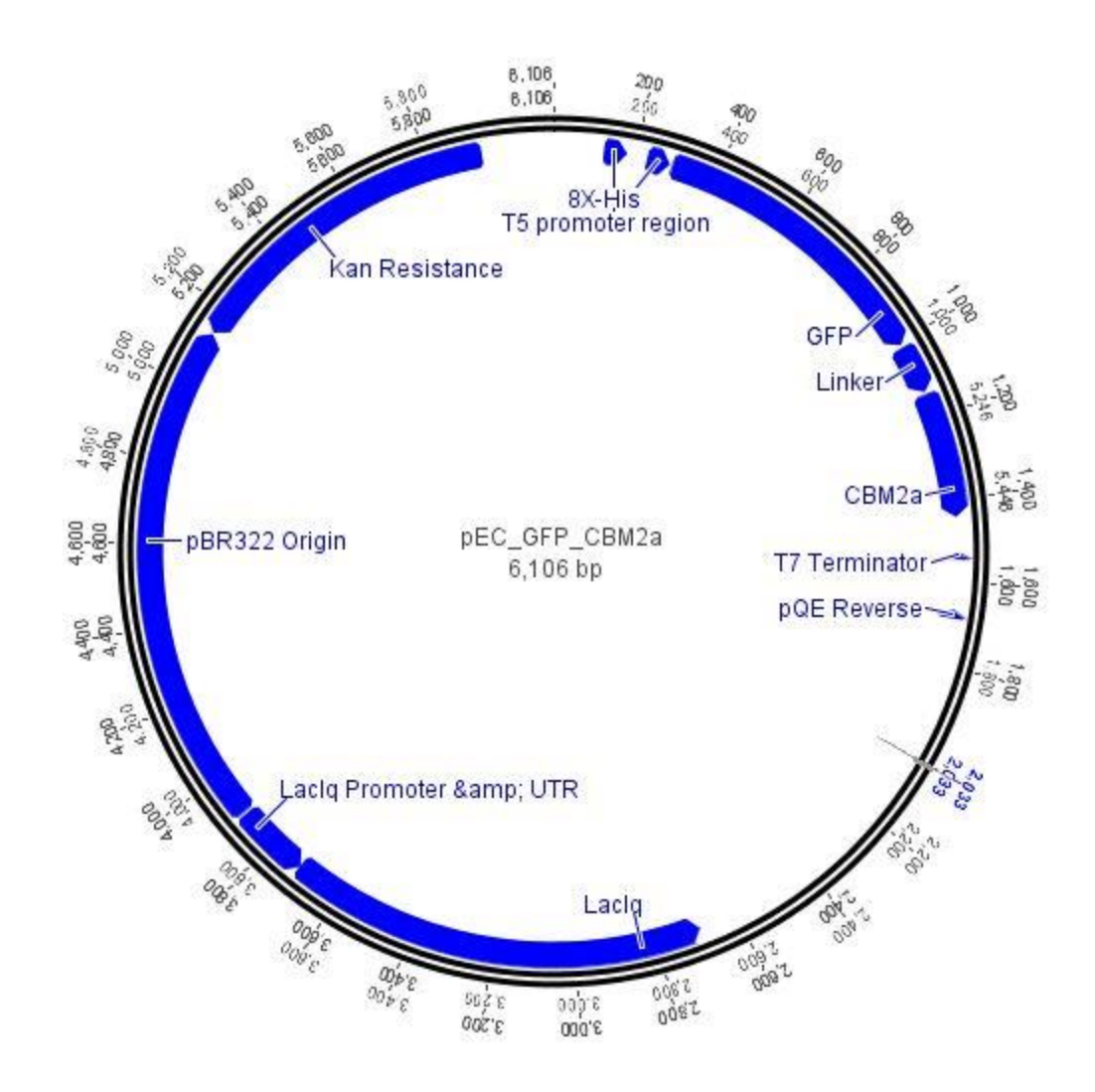


Figure S2: Plasmid map for pEC-GFP-CBM2a: Open reading frame consisting of 8X Histidine tag (labeled 8X-His) followed by GFP, linker and CBM2a wild-type is highlighted. pEC plasmid backbone consists of T5 promoter region and T7 terminator region as described elsewhere¹. Other elements highlighted here are: pBR322 origin of replication, LacI promoter and gene to enable lactose-inducible expression.

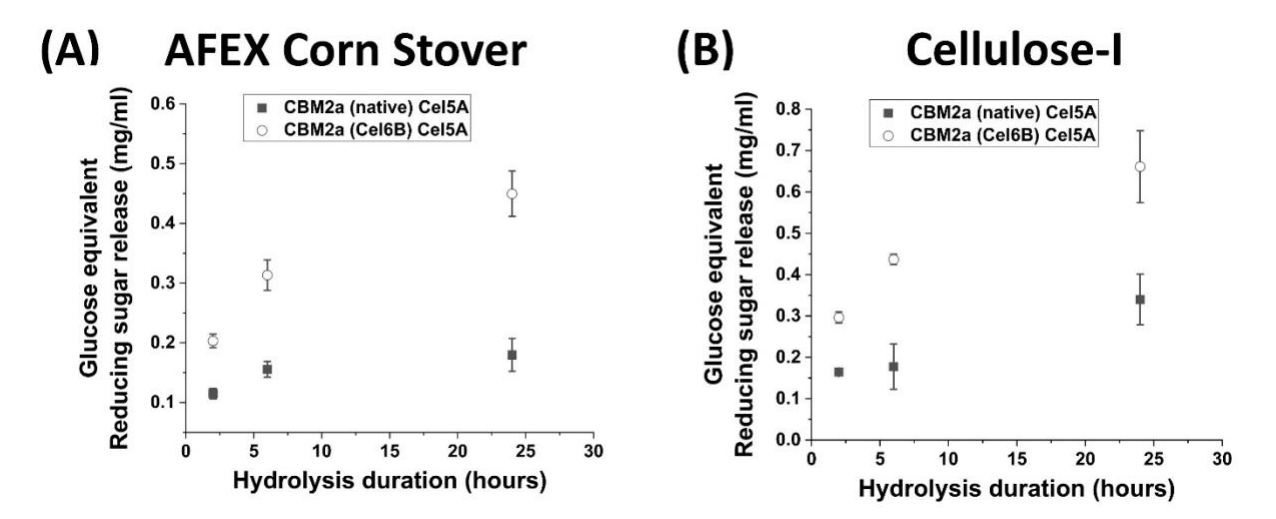


Figure S3: Comparison of CBM2a (native) Cel5A and CBM2a (Cel6B) Cel5A activities towards AFEX Corn Stover and Cellulose-I. 80 μL of 25 g/L AFEX Corn Stover (A) or 40 μL of 100 g/L Avicel Cellulose-I (B) was hydrolyzed using an enzyme loading of 120 nmol CBM2a Cel5A fusion enzyme per gram biomass substrate with 12 nmol β-glucosidase enzyme (10% of cellulase loading) per gram biomass substrate for reaction times of 2hrs, 6hrs, and 24hrs. The solubilized reducing sugar concentrations in the supernatant after hydrolysis were determined by the DNS assay. Glucose equivalent reducing sugar release (mg/ml) as a function of time (2 hr, 6 hr and 24 hr) for the hydrolysis of AFEX Corn Stover and Avicel Cellulose-I by D1 – D8 CBM2a Cel5A and WT CBM2a Cel5A are reported in (A) and (B) respectively. Error bars represent standard deviation from the mean, based on at least 4 replicates.

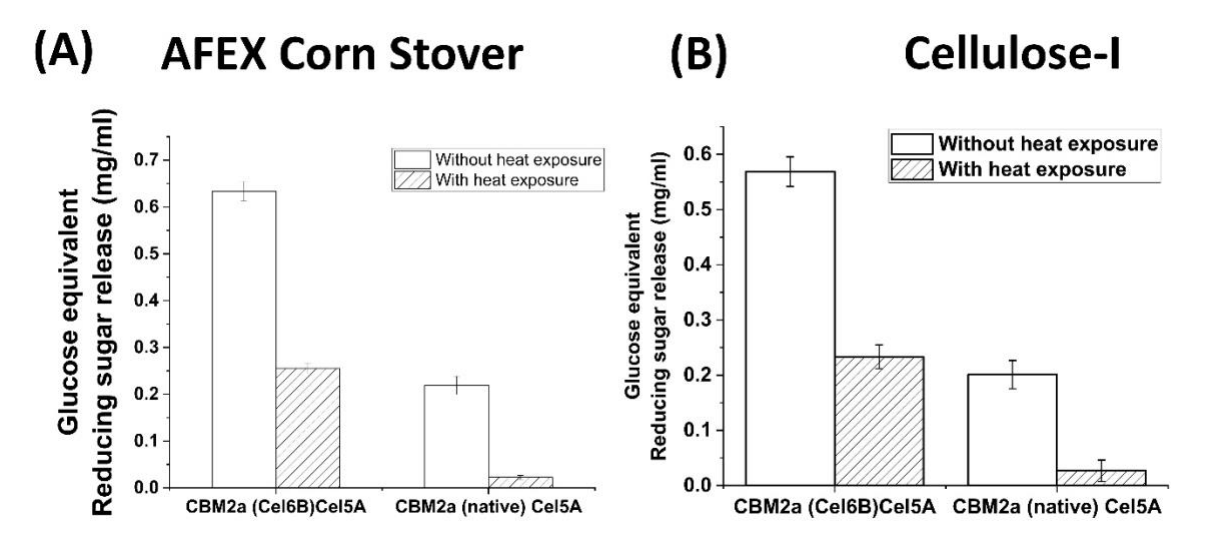


Figure S4: Hydrolytic activity of CBM2a (native) Cel5A and CBM2a (Cel6B) Cel5A towards AFEX Corn Stover and Cellulose-I, upon thermal denaturation at 70 °C Cellulase enzyme (0.0048 nmol/μL concentration) was thermally denatured at 70 °C for 30 minutes using an Eppendorf thermocycler. 50 μl of denatured cellulase enzyme was added to either 80 μl of 25 g/L AFEX Corn Stover (A) or 40 μl of Cellulose-I (B) to establish an effective enzyme loading of 120 nmol enzyme per gram AFEX Corn Stover or Cellulose-I substrate. 12 nmol of β-glucosidase enzyme (10% of cellulase loading) per gram substrate was added to the reaction mixture and incubated at 60 °C for 24 hours. A control reaction was performed with enzyme that was incubated on an ice bath (0 °C) for 30 minutes. The results of enzyme activity upon thermal denaturation at 70 °C are labelled as 'With heat exposure' and those without thermal denaturation are labelled as 'Without heat exposure'. At least 3 replicates were run for each condition and the error bars represent standard deviation from the mean. Reducing sugar yields from hydrolysis of AFEX Corn Stover are reported in (A) and those from Avicel cellulose-I are reported in (B)

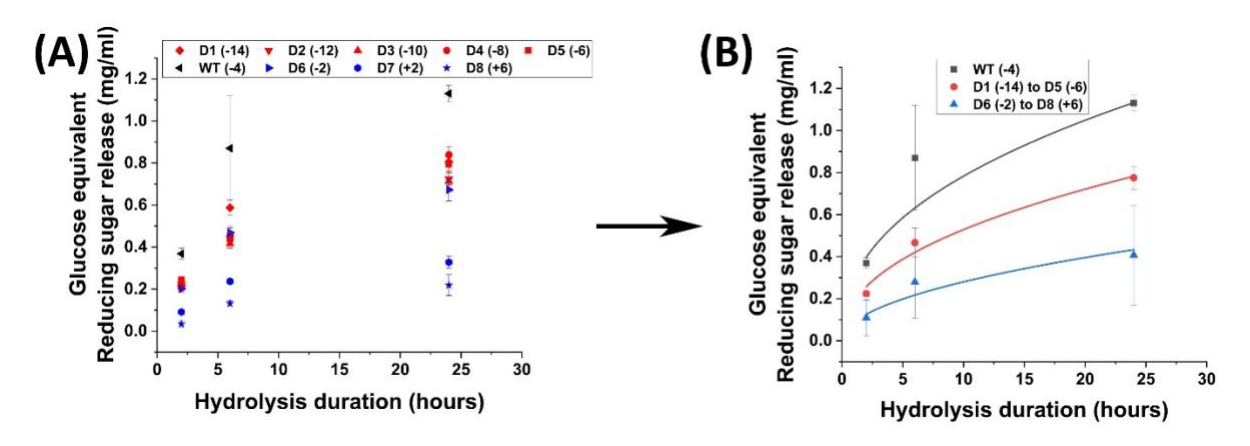


Figure S5: Hydrolytic activity of supercharged cellulases towards EA Corn Stover. 80 μL of 25 g/L EA Corn Stover was hydrolyzed using an enzyme loading of 120 nmol CBM2a Cel5A fusion enzyme per gram biomass substrate with 12 nmol β-glucosidase enzyme (10% of cellulase loading) per gram biomass substrate for reaction times of 2hrs, 6hrs, and 24hrs. The solubilized reducing sugar concentrations in the supernatant after hydrolysis were determined by the DNS assay (A) Glucose equivalent reducing sugar release (mg/ml) as a function of time (2 hr, 6 hr and 24 hr) for the hydrolysis of EA Corn Stover by D1 – D8 CBM2a Cel5A and WT CBM2a Cel5A. Error bars represent standard deviation from the mean, based on at least 4 replicates. (B) Based on the data reported in (A), CBM2a Cel5A fusion constructs with negatively supercharged CBMs (D1 – D5) were grouped together and average hydrolysis yields were obtained for the group, with the error bars representing standard deviation from the mean. Similarly, CBM2a-Cel5A fusion constructs with positively supercharged CBMs (D6 – D8) were grouped together and average hydrolysis yields were obtained. Trend curves have been added to represent the kinetic profiles of the hydrolysis reaction. Wild-type CBM2a-Cel5A is referred to as WT throughout this figure.

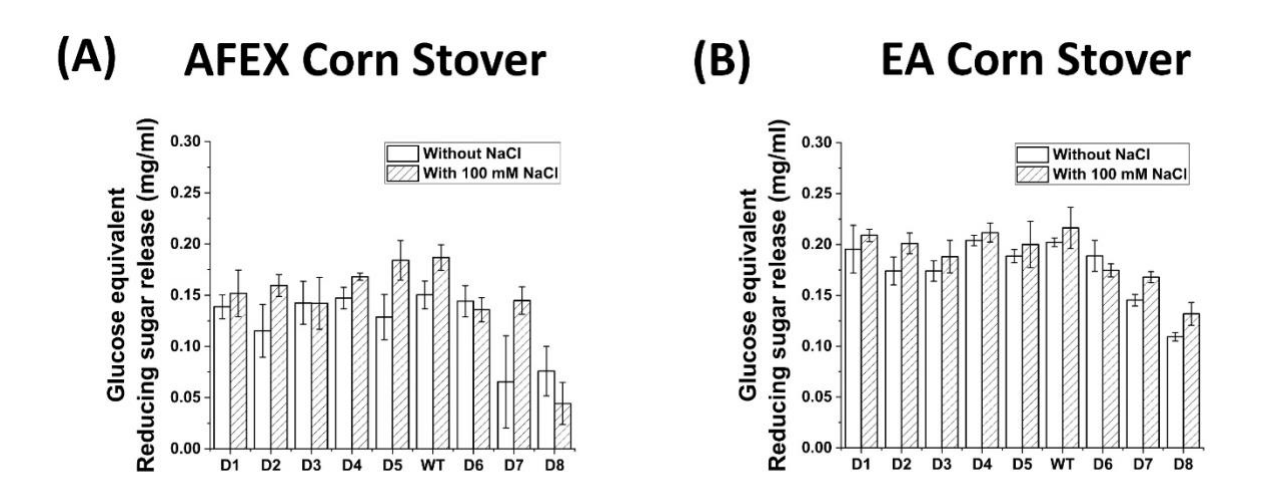


Figure S6: Impact of salt on hydrolysis of AFEX and EA Corn Stover by mutant enzymes. $80~\mu L$ of 25~g/L AFEX or EA Corn Stover was hydrolyzed using an enzyme loading of 120~nmol CBM2a Cel5A fusion enzyme per gram biomass substrate with 12~nmol β -glucosidase enzyme (10% of cellulase loading) per gram biomass substrate for a reaction time of 2~hours. For reactions to be carried out in the presence of NaCl, $20~\mu l$ of 1M~NaCl was added to a total reaction volume of $200~\mu l$ resulting in an effective NaCl concentration of 100~mM. The solubilized reducing sugar concentrations in the supernatant after hydrolysis were determined by the DNS assay for AFEX corn stover (A) and EA corn stover (B). Wild-type CBM2a-Cel5A is referred to as WT throughout this figure.

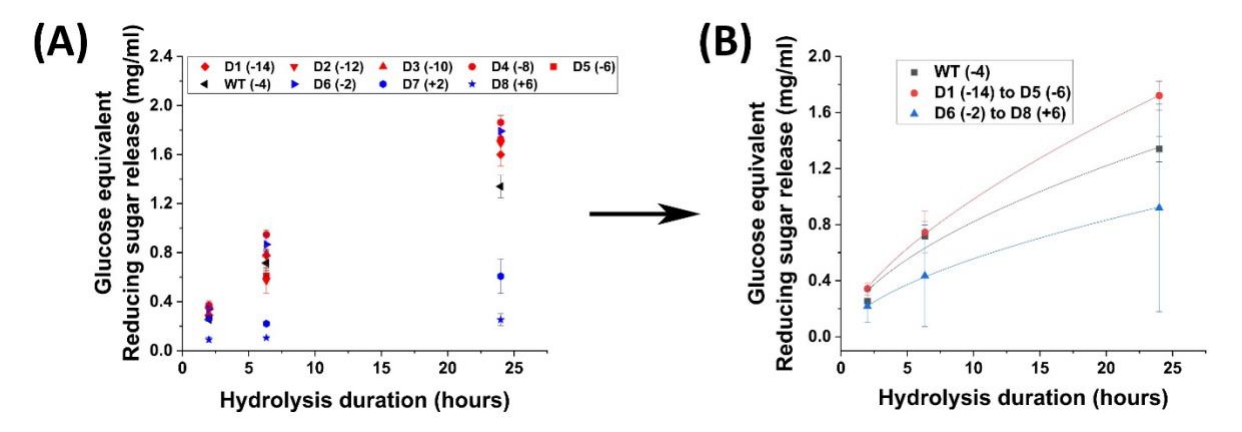


Figure S7: Hydrolytic activity of supercharged cellulases towards Avicel Cellulose-III. 40 μ L of 100 g/L Avicel cellulose-III substrate was hydrolyzed using an enzyme loading of 120 nmol CBM2a Cel5A fusion enzyme per gram cellulose substrate supplemented with 12 nmol of β-glucosidase enzyme (10% of cellulase loading) per gram cellulose substrate for reaction times of 2hrs, 6hrs, and 24hrs. The solubilized reducing sugar concentrations in the supernatant after hydrolysis were determined by the DNS assay (A) Glucose equivalent reducing sugar release (mg/ml) as a function of time (2 hr, 6 hr and 24 hr) for the hydrolysis of Cellulose-III by D1 – D8 CBM2a Cel5A and WT CBM2a Cel5A. Error bars represent standard deviation from the mean, based on at least 4 replicates. (B) Based on the data reported in (A), CBM2a Cel5A fusion constructs with negatively supercharged CBMs (D1 – D5) were grouped together and average hydrolysis yields were obtained for the group, with the error bars representing standard deviation from the mean. Similarly, CBM2a-Cel5A fusion constructs with positively supercharged CBMs (D6 – D8) were grouped together and average hydrolysis yields were obtained. Trend curves have been added to represent the kinetic profiles of the hydrolysis reaction. Wild-type CBM2a-Cel5A is referred to as WT throughout this figure.

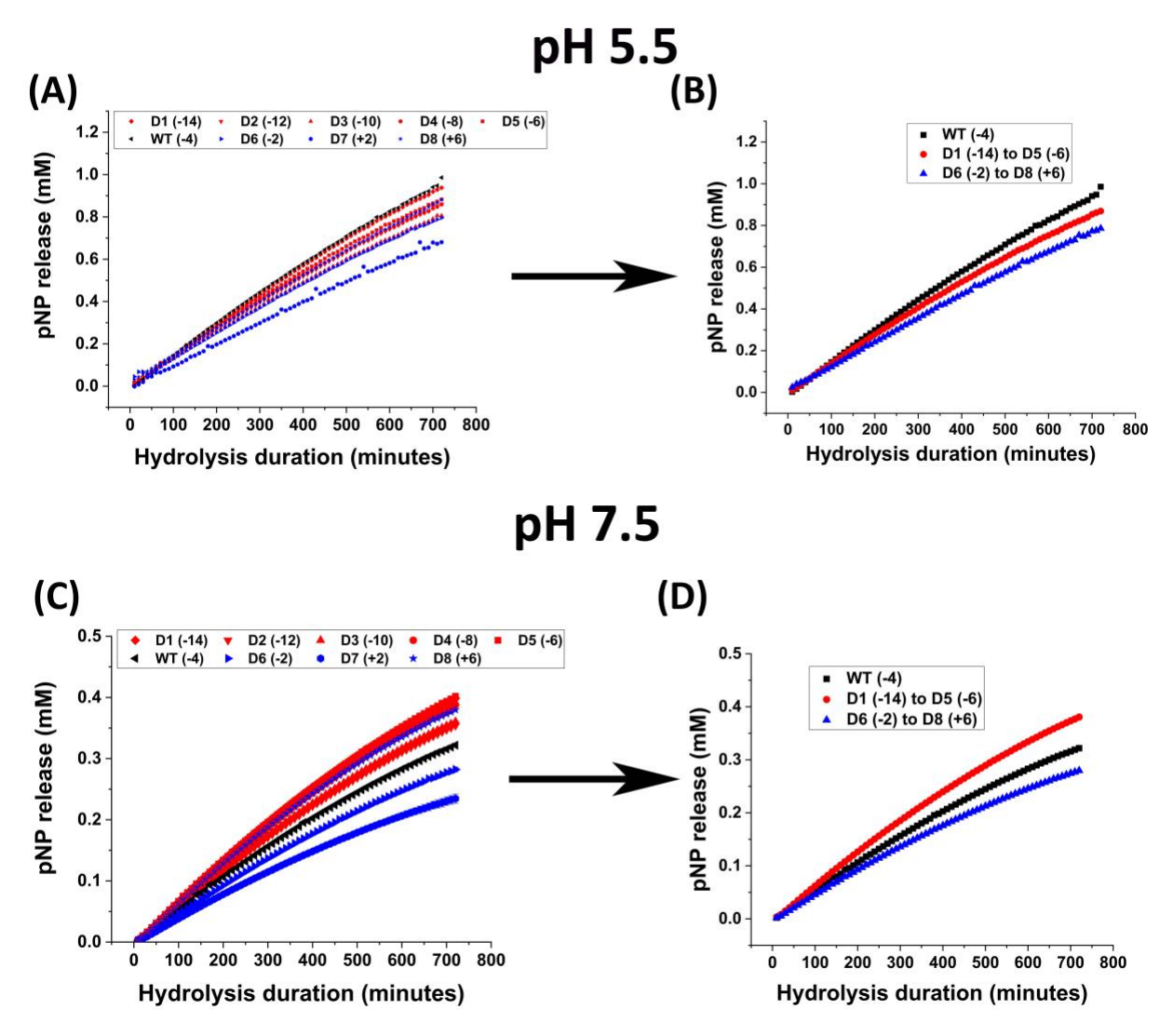


Figure S8: Enzyme mutant activity towards pNPC. Hydrolysis assays were performed by mixing 100 μl pNPC slurry (2 mM), 7.5 μl 1 M sodium acetate buffer pH 5.5 or 7.5 μl 1 M MOPS (pH 7.5), 42.5 μl cellulase enzyme (at an appropriate concentration to constitute 5 ug of enzyme per g pNPC) in a microplate and measuring pNP absorbance via a UV-Vis spectrophotometer, as laid out in *Whitehead et al.* (2017). (A) Raw data for pNPC hydrolysis response by supercharged enzymes at pH 5.5 (B) Average pNP hydrolysis by negatively supercharged sub-group (D1 – D5) and positively supercharged sub-group (D6 – D8) based on raw data reported for pH 5.5 in 'A' (C) Raw data for pNPC hydrolysis response by supercharged enzymes at pH 7.5 (D) Average pNP hydrolysis by negatively supercharged sub-group (D1 – D5) and positively supercharged sub-group (D6 – D8) based on raw data reported for pH 7.5 in 'C'.

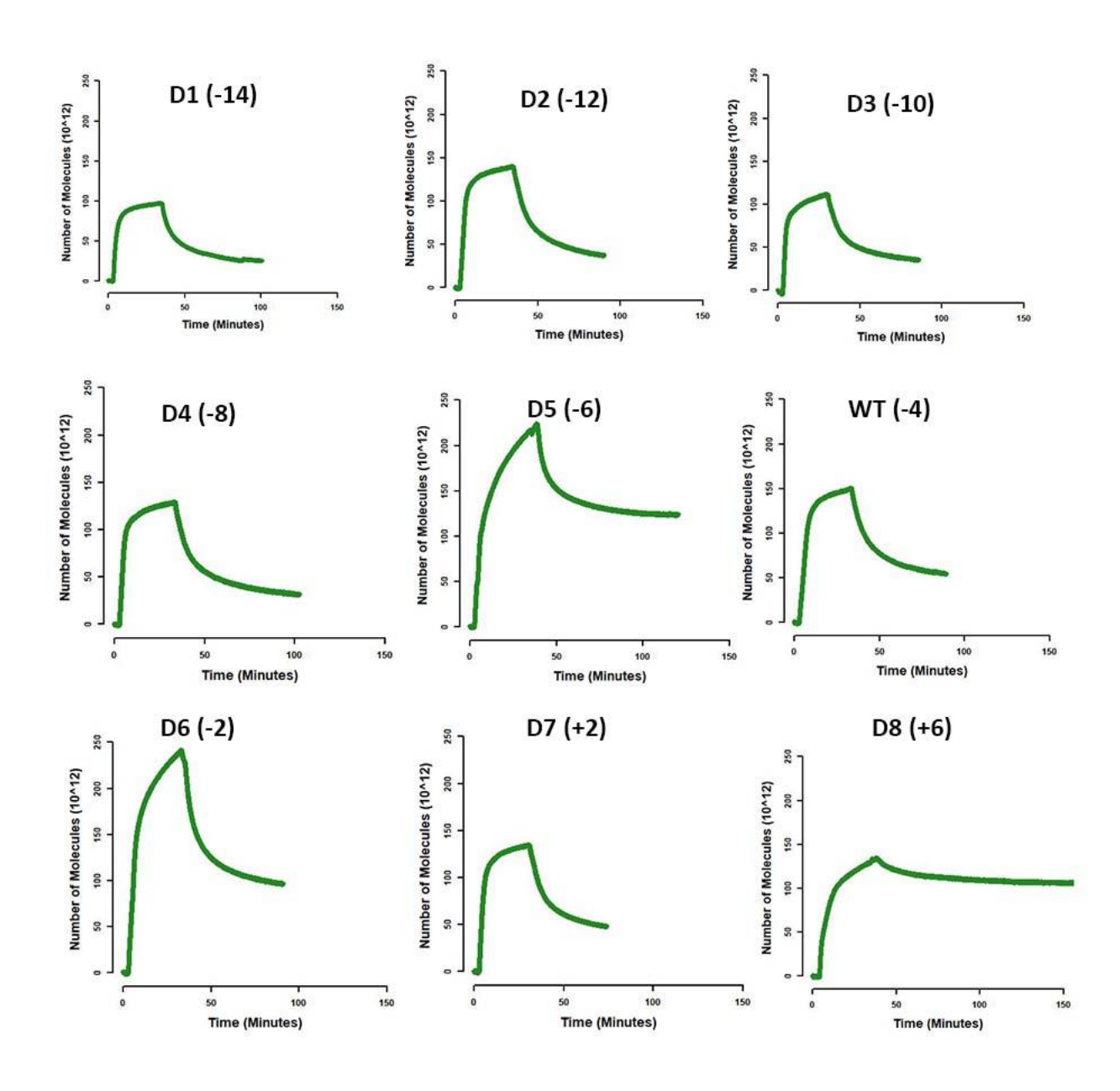


Figure S9: Binding-unbinding QCM-D representative sensorgrams for GFP-CBM2a designs binding to crystalline cellulose I. Sensorgrams obtained from Quartz crystal microbalance with dissipation (QCM-D) for binding of GFP-CBM2a designs to cellulose-I were converted to number of molecules * (10^{12}) vs time (minutes) using the Sauerbrey equation. These curves were then used to obtain the kinetic parameters for binding and unbinding as reported in **Table 1** of the main manuscript. The equations used for curve fitting have been reported previously in *Nemmaru et al.* (2020).

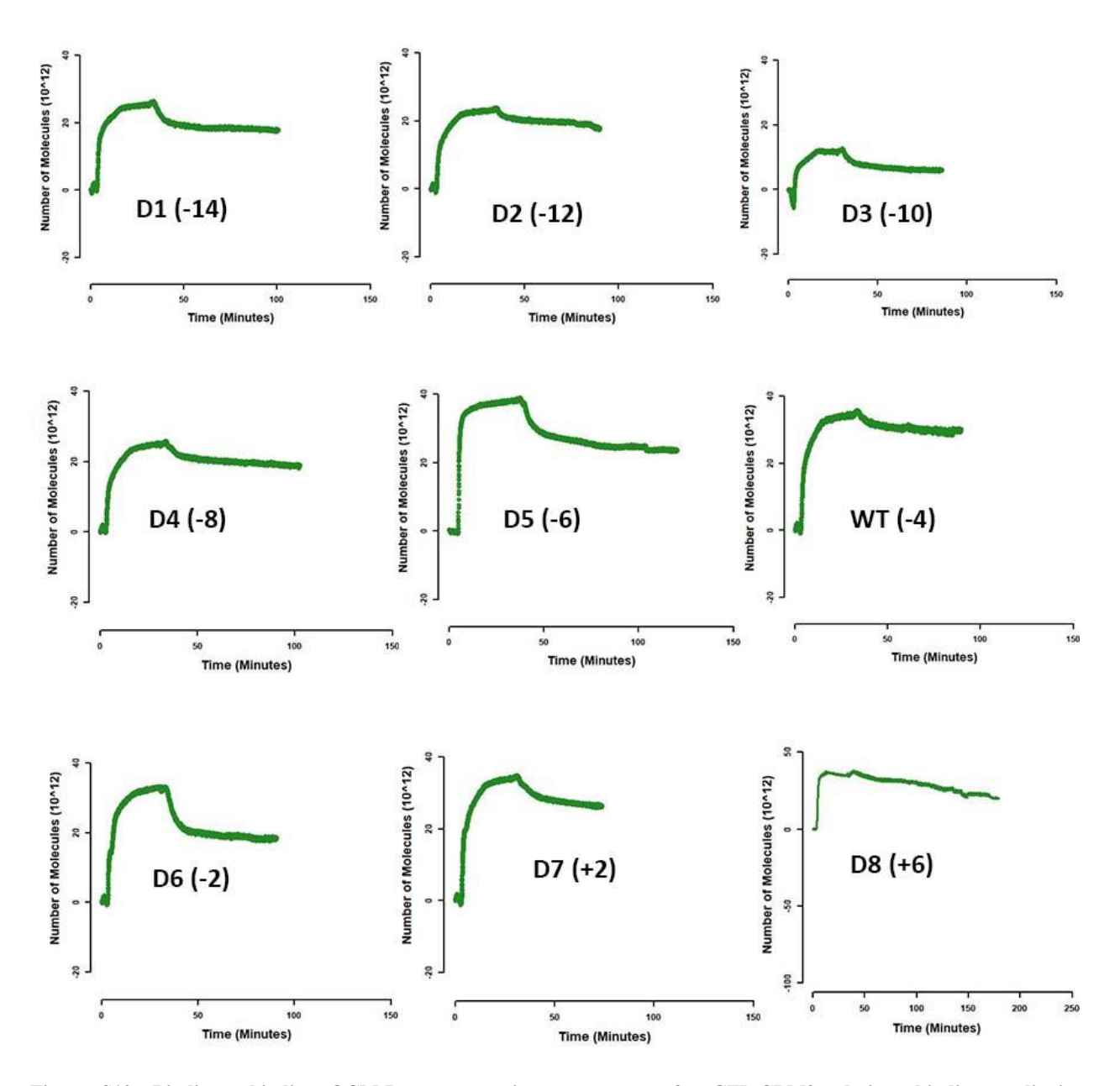


Figure S10: Binding-unbinding QCM-D representative sensorgrams for GFP-CBM2a designs binding to lignin. Sensorgrams obtained from Quartz crystal microbalance with dissipation (QCM-D) for binding of GFP-CBM2a designs to lignin were converted to number of molecules * (10^{12}) vs time (minutes) using the Sauerbrey equation. Due to irreversible binding of CBM2a mutants to lignin, the total number of binding sites and percentage of protein recovered were the only two parameters that could be inferred (see SI Appendix Table T7).

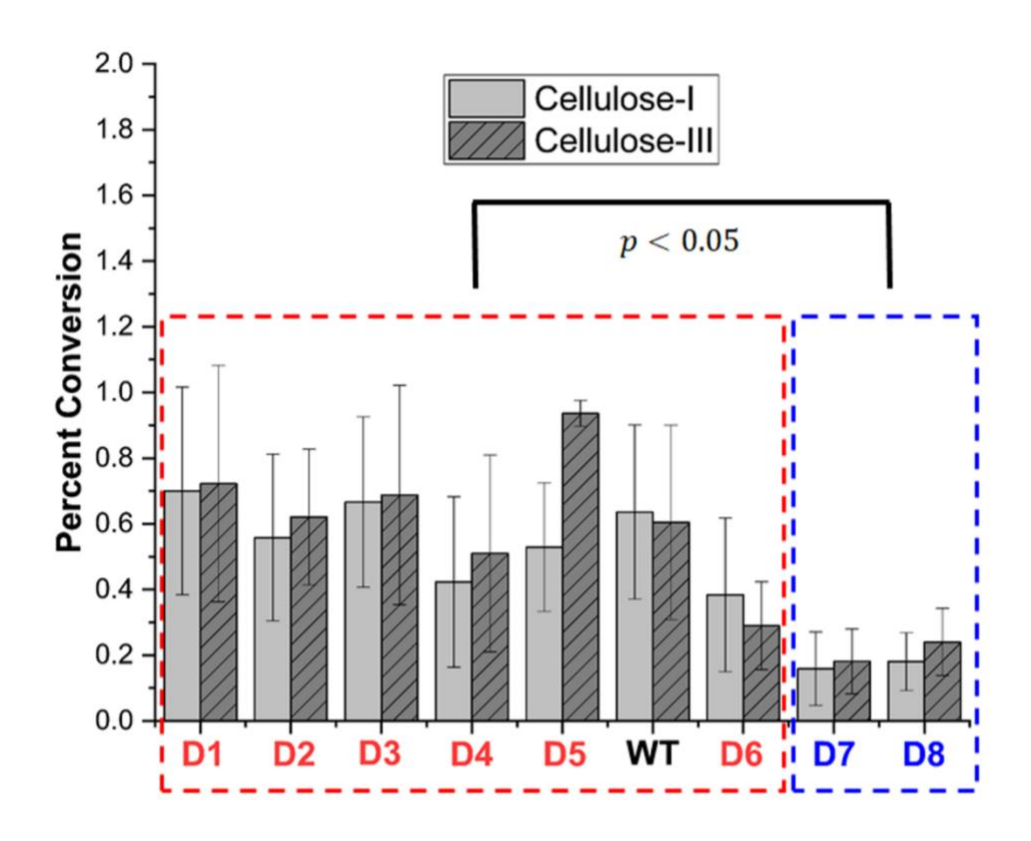


Figure S11: Lignin-mediated inhibition of enzyme activity towards Cellulose-I and Cellulose-III. 20 μ L of 100 g/L of Avicel Cellulose-I (light gray) or Avicel Cellulose-III (dark gray with lines) with addition of 80 μ L of 25g/L dioxane extracted corn stover lignin was hydrolyzed using an enzyme loading of 120 nmol CBM2a Cel5A fusion enzyme per gram cellulose substrate and 12 nmol β-glucosidase per gram cellulose substrate for 24 hours. The solubilized reducing sugar concentrations in the supernatant after hydrolysis were determined by the DNS assay. Percent conversion of cellulosic substrate to glucose equivalents is reported on the Y-axis. T-test analysis (reported in the SI Appendix) was done to show that the activity of the fusion constructs with negatively charged CBMs (red box) is statistically significantly different from that of the fusion constructs with positively charged CBMs.

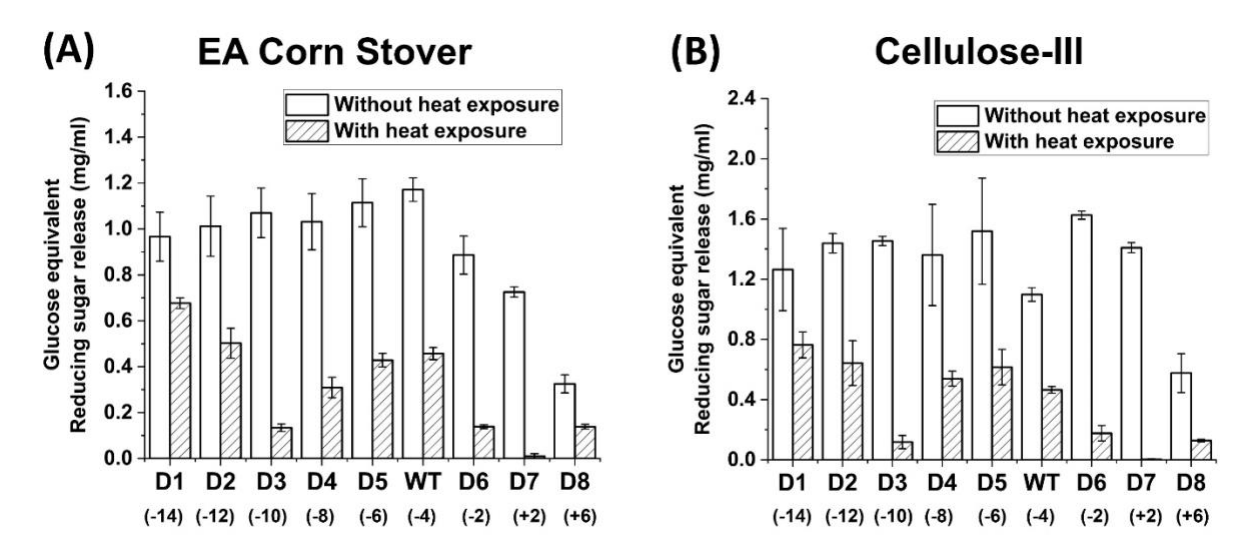


Figure S12: Impact of thermal treatment at 70 °C on enzyme activity towards EA Corn Stover (A) and Cellulose-III (B). Cellulase enzyme (0.0048 nmol/ μ L concentration) was thermally denatured at 70 °C for 30 minutes using an Eppendorf thermocycler. 50 μ l of denatured cellulase enzyme was added to either 80 μ l of 25 g/L EA Corn Stover (A) or 40 μ l of Cellulose-III (B) to establish an effective enzyme loading of 120 nmol enzyme per gram EA Corn Stover or Cellulose-III substrate. 12 nmol of β-glucosidase enzyme (10% of cellulase loading) per gram substrate was added to the reaction mixture and incubated at 60 °C for 24 hours. A control reaction was performed with enzyme that was incubated on an ice bath (0 °C) for 30 minutes. The results of enzyme activity upon thermal denaturation at 70 °C are labelled as 'With heat exposure' and those without thermal denaturation are labelled as 'Without heat exposure'. At least 3 replicates were run for each condition and the error bars represent standard deviation from the mean. Reducing sugar yields from hydrolysis of EA Corn Stover are reported in (A) and those from Avicel cellulose-III are reported in (B).

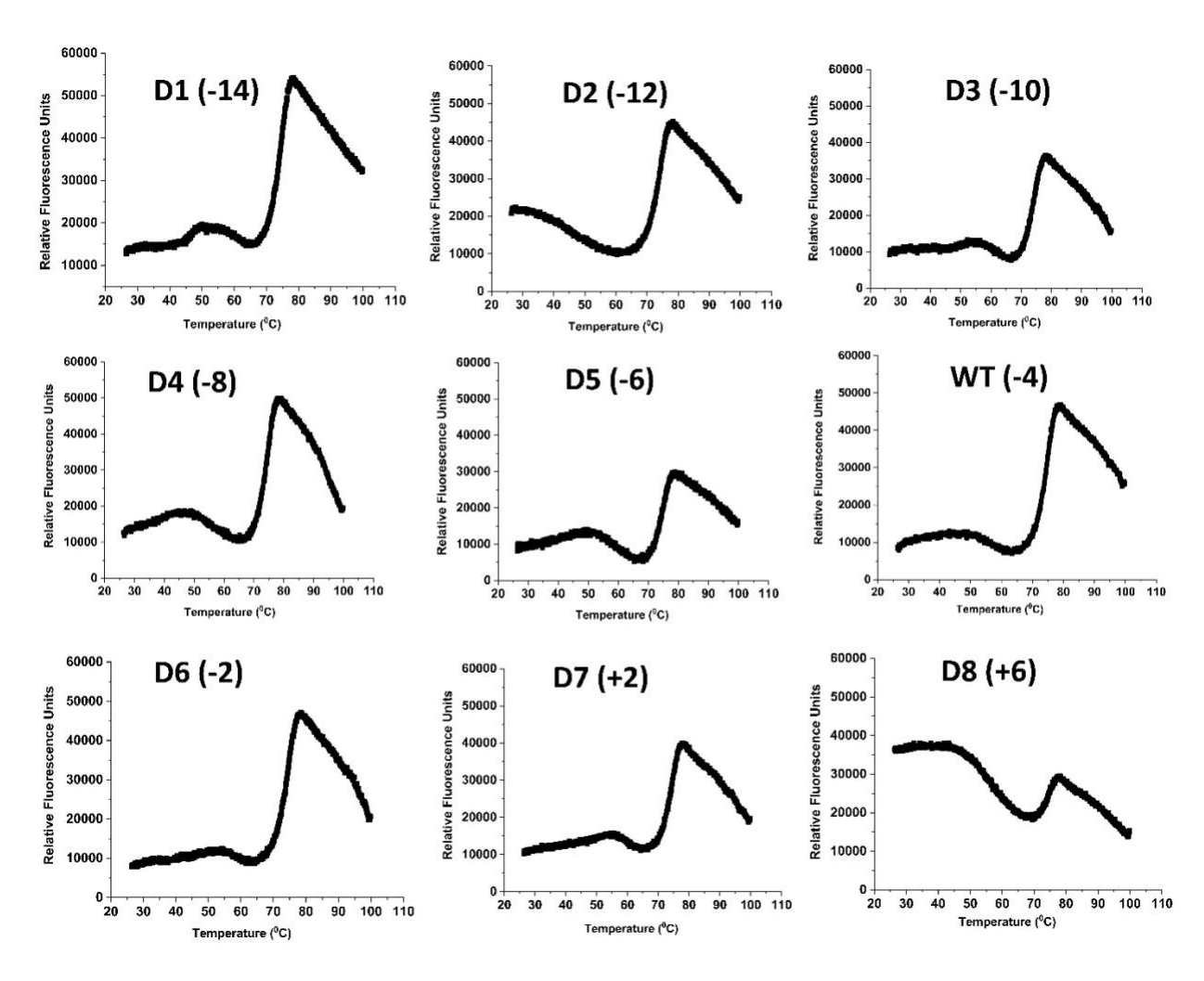


Figure S13: Representative melt curves from thermal shift assay 5 μl 200X SYPRO reagent, 5 μl 0.5 M sodium acetate buffer (pH 5.5), enzyme dilution to make up an effective concentration of 5 μM and deionized water to make up the total volume to 50 μl were added to MicroAmpTM EnduraPlateTM 96-well clear microplate (Applied BiosystemsTM) and fluorescence (excitation – 470 nm; emission – 520 nm) was measured using QuantStudio3 under the FAM dye channel. Representative curves for each CBM2a-Cel5A fusion construct are reported here, starting from D1 (-14 net charge) up to D8 (+6 net charge) including the wild-type (-4 net charge).

REFERENCES:

 Blommel, P. G., Martin, P. A., Seder, K. D., Wrobel, R. L. & Fox, B. G. Flexi Vector Cloning. in *High Throughput Protein Expression and Purification: Methods and Protocols* (ed. Doyle, S. A.) 55–73 (Humana Press, 2009). doi:10.1007/978-1-59745-196-3 4